



Universitetet  
i Stavanger

DET TEKNISK-NATURVITENSKAPELIGE FAKULTET

## MASTEROPPGAVE

Studieprogram/spesialisering: Petroleum Engineering/Reservoir technology	Vårsemesteret, 2014  Åpen / Konfidensiell
Forfatter: Eirik Haugvaldstad	..... (signatur forfatter)
Fagansvarlig:  Veileder(e): Skule Strand, Tina Puntervold	
Tittel på masteroppgaven:  Engelsk tittel: Clay minerals in sandstone reservoirs: implications for «smart water» injection	
Studiepoeng: 30	
Emneord: -Clay minerals -«Smart Water» -EOR -Cation exchange capacity -Wettability	Sidetall: .....  + vedlegg/annet: .....  Stavanger, 16.06.2014 dato/år

Clay minerals in sandstone reservoirs:  
implications for “smart water” injection

June 16, 2014

Master Thesis by Eirik Haugvaldstad

University of Stavanger

Spring 2014

## Acknowledgments

First and foremost I would like to extend my deepest gratitude to my supervisors, Skule Strand and Tina Puntervold. They have included me in a very interesting field of research, a field which encourages us to push the limits of knowledge and technology, and to manage our natural resources in an efficient manner. As good supervisors often do, they knew exactly when to guide and when to leave me to my own devices. I appreciate their honesty and constructive criticism in the instances where I had unknowingly betrayed my research objectives or started down a dead end.

This thesis, like so many before it, is the product of long hours, hair-pulling frustration, academic curiosity, determination, and coffee. During work on this project I have learned more than I ever imagined there was to know about clay minerals, and for that I would like to thank my geological spirit guide, Paul Nadeau. His contributions, in the forms of helpful discussion and relevant reading material, have been invaluable to me and I consider myself lucky for having had his expertise at my disposal. I am especially thankful for the encouragement I have received from my friends, family, and girlfriend over these past months. It has helped me to push onwards whenever I felt overwhelmed, stupid, or simply lazy. Lastly I would like to thank my good friends Thomas Danielsen and Einar Thodal for making this thesis readable. Their skeptical gaze has helped me remove what I hope was most of my spelling errors and bad writing. Thank you all.

## Abstract

Clay minerals are ubiquitous in sandstone reservoirs, yet many of their effects are not well understood. This literature study examines the relationship between the most common clay minerals and “smart water” injection in sandstone reservoirs. Ion exchange capacities, wettability, and reservoir quality are examined as functions of origin, morphology, chemical properties, and particle size of clay minerals. Authigenic clay minerals are found to have severe consequences for reservoir quality, especially in deeply buried reservoirs. Diagenetic processes, like illitization and chlorite coating can reduce permeability and porosity to the point where production becomes impossible, while kaolinite can contribute to more favorable initial wetting conditions. Cation exchange capacity can vary significantly due to effects of particle size and pH, affecting adsorption/desorption of polar oil components, both in the reservoir and in core flood experiments. It will also be shown that fibrous clay morphologies, common for illites and smectites, collapse during air-drying, leaving core samples unrepresentative with regards to their native state. Steps such as critical point drying should be taken to preserve these morphologies when using core floods to simulate “smart water” injection. Further study of wetting properties related to morphology and isomorphous substitution, as well as more thorough characterizations of common phyllosilicates is suggested. The role of anionic exchange capacity in adsorption/desorption reactions for kaolinite and chlorite may also warrant a closer look.

# Contents

<b>1</b>	<b>Introduction</b>	<b>1</b>
1.1	Background . . . . .	1
1.2	Objectives . . . . .	1
<b>2</b>	<b>Fundamental Theory</b>	<b>2</b>
2.1	Enhanced Oil Recovery . . . . .	2
2.2	Interfacial tension . . . . .	3
2.3	Wettability . . . . .	3
2.4	Displacement forces . . . . .	4
2.4.1	Gravity forces . . . . .	5
2.4.2	Capillary forces . . . . .	5
2.4.3	Viscous forces . . . . .	6
2.4.4	Relationship of displacement forces . . . . .	6
2.5	Oil components . . . . .	7
2.6	Sandstones . . . . .	8
2.7	Clay minerals . . . . .	8
2.7.1	Structure and properties . . . . .	9
2.7.2	CEC and surface reactivity . . . . .	13
2.7.3	Origin . . . . .	14
2.7.4	Diagenesis . . . . .	15
2.8	Water injection . . . . .	16
<b>3</b>	<b>“Low salinity injection” and “smart water”</b>	<b>17</b>
3.1	Conditions for “smart water” effect . . . . .	17
3.2	Proposed mechanisms . . . . .	18
3.2.1	Migration of fines . . . . .	18
3.2.2	pH related to alkaline flooding . . . . .	18
3.2.3	Multi component ion exchange (MIE) . . . . .	19
3.2.4	Expansion of the ionic electrical double layer . . . . .	19
3.2.5	Desorption by pH increase . . . . .	20
<b>4</b>	<b>Results and discussion</b>	<b>21</b>
4.1	Effect of clay minerals on reservoir properties . . . . .	21
4.1.1	Porosity . . . . .	21
4.1.2	Permeability . . . . .	25
4.2	CEC: effects of particle size and pH . . . . .	29
4.3	Initial wetting in sandstone reservoirs . . . . .	36
4.4	Conclusions: “Smart water” injection and pre-flood core studies . . . . .	40
	<b>References</b>	<b>41</b>

# 1 Introduction

## 1.1 Background

In the spring of 2011 the Norwegian Ministry of Petroleum and Energy published a guide entitled “An industry for the future - Norway’s petroleum activities”. In this report the ministry stated that the decline in oil production must be curbed by, among other things, improved recovery and outlined several ways of accomplishing this goal [1]. The need for improved recovery is frequently mentioned in the yearly cooperative report published by the aforementioned ministry and the Norwegian Petroleum Directorate [2]. The expected average oil recovery factor with currently adopted plans for the Norwegian Continental Shelf (NCS) is considerably higher than the global average, 46% vs. 22% [2]. Yet, calculations show that if the recovery factor for all operative Norwegian fields rose by one percent the additional gross income from sales would be approximately 325 billion NOK. [2]. In this context it is clear that even small improvements in EOR techniques could lead to major financial gains. In the last year two new research centers have been established, one at the University of Tromsø, and one at the University of Stavanger, in the hopes of advancing expertise and research in the field of petroleum technology.

“Smart water” injections is one of the promising methods for increased recovery, and the one that this thesis will focus on. Fundamental theoretical concepts will be explained in chapter 2, and will serve as a foundation for further discussion in chapter 4. Chapter 3 will be a summary of the accumulated knowledge of the “low salinity effect” and an introduction to the “smart water” concept.

## 1.2 Objectives

The basis for this thesis is a proposed mechanism for the observed “low salinity effect” in sandstone reservoirs, presented by Austad et al. in 2010 [3]. The researchers who published the paper are currently running experiments for further publications on the subject. They requested a literature study on clay minerals and their effect on the potential for injection of specially tailored injection water, or “smart water”, in sandstone reservoirs. Mechanisms governing the interactions between different clay minerals, brine, oil, and reservoir rock will be examined and explained. Additionally, the effect of clay minerals on reservoir quality and wetting properties will be linked to their origin and characteristics. Special attention will be given to the aspects of morphology and particle size, and to how this relates to variation in surface reactivity and Cation Exchange Capacity (CEC). Because of their relative abundance on the NCS [4], kaolinite, illite, and chlorite will be the primary subjects of study, but montmorillonite will also be included.

## 2 Fundamental Theory

### 2.1 Enhanced Oil Recovery

Due to the clarity and simplicity of its explanation, this paragraph is inspired by the book “Enhanced Oil Recovery” [5]. Traditionally, oil recovery processes have been divided into three separate categories. The first of these categories is called primary oil recovery. During this period of production oil is expelled from the reservoir and towards the production well by the energy stored in the reservoir alone. In other words, the inherent pressure energy in the reservoir drives the oil recovery process. The second traditional category, called secondary recovery, is usually implemented after the primary production period, when the pressure of the reservoir is no longer high enough to yield the desired production rates. During this process, pressure management, gas injection, and waterflooding can be used to sustain oil production rates. Tertiary recovery is the third category, which was traditionally applied after the secondary recovery became uneconomical. Flooding with chemicals, such as surfactants and polymers, injection of miscible gases, and the use of thermal energy can all be classified as tertiary recovery methods in the traditional model. It should be noted that although primary, secondary, and tertiary refer to the chronological order of their application they are not necessarily utilized in that order. Many reservoirs may not benefit from one or more of the traditional recovery processes, and may only be subject to processes from one of the categories. A good example of this would be the extraction of heavy oil, where steam injection and other thermal processes are used to mobilize the viscous oil. In such reservoirs the oil does not flow under normal reservoir conditions and primary recovery would be uneconomical.

As a result of these chronological inconsistencies, the methods traditionally classified as tertiary recovery processes are now mostly referred to as enhanced oil recovery (EOR) processes. The purpose of EOR processes is to increase recovery, by increasing microscopic displacement efficiency, and/or increasing volumetric sweep efficiency. Definitions of these two quantities are given by the equations (1) and (2).

$$E_D = \frac{S_{oi} - S_{or}}{S_{oi}} \quad (1)$$

Where

$E_D$  is the microscopic displacement efficiency

$S_{oi}$  is the initial oil saturation

$S_{or}$  is the residual oil saturation in the parts of the reservoir contacted by the displacing fluid.

$$E_V = E_I * E_A \quad (2)$$

Where

$E_V$  is the volumetric sweep efficiency

$E_I$  is the vertical sweep efficiency

$E_A$  is the areal sweep efficiency.

The sweep efficiencies  $E_I$  and  $E_A$  are the fractions of the reservoir that have been contacted by the displacing fluid in the vertical and areal planes respectively.  $E_V$  is the product of the two, and is the volume fraction of the reservoir that has been swept by the displacing fluid. As we can see from (1), the microscopic displacement efficiency depends on the residual oil saturation. The goal of EOR processes such as surfactant injection is to decrease the residual oil saturation in the contacted regions of the reservoir, thereby increasing the microscopic displacement efficiency and oil recovery. The residual oil saturation is itself dependent on the viscous and capillary forces that govern trapping and mobilization of fluids in a porous medium. An explanation of these forces will be given in section 2.4.

## 2.2 Interfacial tension

Interfacial tension is related to the forces and surface energy that exist at the interface between two immiscible phases in contact with each other. This energy influences fluid distributions, saturations, and displacement processes. The molecules of a phase attract each other due to cohesive forces, and a molecule that is positioned within the bulk of the phase will experience an equal pull in all directions. However, a molecule that exists at or near the interface between the two immiscible phases will experience a net force pulling the molecule back into the bulk of the phase since the attractive forces are no longer balanced. To easier visualize interfacial tension, the interface can be seen as an elastic membrane, where the shape is dependant on the surface energy. The net force acting on the molecule at the interface shortens the membrane, and additional energy is required to stretch it. Interfacial tension can then be defined as the force per unit length that is needed to stretch the interface, increasing its area [5].

## 2.3 Wettability

Wettability can be said to be the tendency of one fluid to spread on and adhere to a surface in the presence of another fluid [5]. Usually, when two immiscible phases are in contact with a solid surface, one of the fluids will show a stronger attraction to the surface than the other [5]. The more strongly attracted fluid is designated the wetting phase and the rock is either water-wet or oil-wet. In some cases different states will exist, either because some parts of the rock are water-wet while other parts are oil-wet, or because the surfaces are not strongly wet by either of the fluids. These states are usually termed intermediate wetting and mixed wetting, respectively [7]. States of wettability are not binary, but lie on a continuum where strongly oil-wet and strongly water-wet are the endpoints.



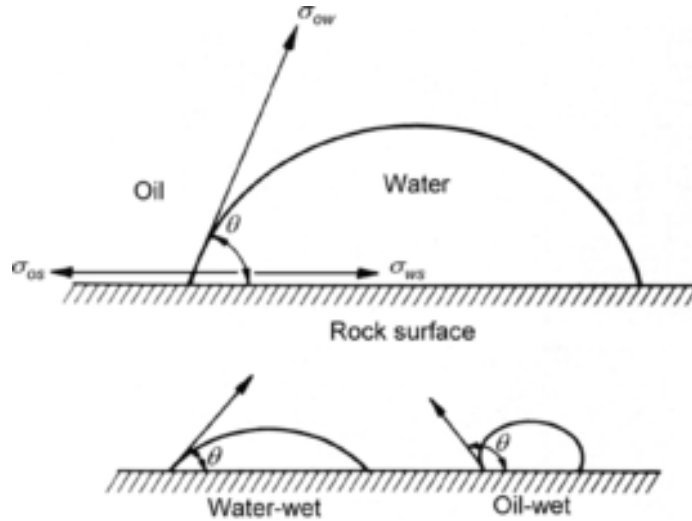


Figure 1: Wettability of oil/water/rock system. Figure from [6].

When the rock is oil-wet there is a tendency for oil to occupy the smallest pores and to contact the majority of the rock surface, while in a water-wet system this preference will be reversed. Wettability of an oil/water/rock system is shown in figure 1. Note that the wetting angle  $\theta$  is measured through the water phase. Sandstone reservoirs are initially strongly water-wet, but may develop a more complex wettability when filled with migrating oil. The reason for this wettability alteration will be covered by section 2.5. Wettability of the fluid/rock system heavily influences flow, distribution, and location of the fluids in a reservoir [8]. For optimum recovery by “smart water” flooding, weakly water-wet (close to neutral wetting) seems to be the preferred initial state [9]. The wetting state of the reservoir before it is disturbed by human interventions is designated as the initial wetting. A more comprehensive discussion of the initial wettability state of the reservoir will be carried out in chapter 4. When simulations of displacement processes are carried out in a laboratory, the wetting state of the cores should be matched as closely as possible to reservoir wetting for representative results.

## 2.4 Displacement forces

Fluids in a reservoir are subjected to a wide range of forces of varying direction and magnitude. The most important ones are gravity forces, capillary forces, and viscous forces. In this section the forces will be defined and briefly discussed.

### 2.4.1 Gravity forces

Gravity forces arise from the different densities of the fluid phases, with larger differences in density producing stronger gravity forces. Buoyancy is the concept that governs the direction and magnitude of the resultant force on a given phase. The relation for buoyancy is given in equation (3). The consequence of the relation is that the lighter phase will experience an upwards pressure, causing segregation of the two immiscible phases. During immiscible displacement processes this segregation can lead to unwanted effects. If the injected fluid is less dense than the displaced fluid, as is the case in CO<sub>2</sub> flooding, the segregation leads to gravity override, where the injected fluid flows on top of the displaced fluid. For waterfloods the opposite effect occurs, and the segregation leads to gravity underdrive. Both these effects lead to early breakthrough of the injected fluid and reduced vertical sweep efficiency [5]. However, they can also be used to increase the efficiency of the displacement when flooding in an up-dip or down-dip direction [5].

$$\Delta P_g = \Delta \rho g H \quad (3)$$

Where

$\Delta P_g$  is the pressure difference over the interface due to gravity

$\Delta \rho$  is the difference in density between the two phases

$g$  is the gravitational acceleration constant, equal to 9,81 m/s<sup>2</sup>

$H$  is the height of the fluid column

### 2.4.2 Capillary forces

Capillary pressure is the pressure difference that exists across the curved interface between two immiscible phases due to the tension of the interface [5]. It is defined as the pressure in the non-wetting phase minus the pressure in the wetting phase, or by convention, as the pressure in the oil phase minus pressure in the water phase. The larger pressure exists in the non-wetting phase [5]. Using the conventional definition it becomes apparent that the capillary pressure can be positive or negative, depending on which phase wets the solid surface. The Young-Laplace equation for capillary pressure can be written as:

$$P_c = P_o - P_w = \sigma_{ow} \left( \frac{1}{R_1} + \frac{1}{R_2} \right) \quad (4)$$

Where

$P_c$  is the capillary pressure

$P_o$  is the pressure in the oil phase

$P_w$  is the pressure in the water phase

$\sigma_{ow}$  is the interfacial tension for oil and water

$R_1, R_2$  are the radii of curvature for the interface.

For capillary rise in a thin tube the capillary pressure becomes:

$$P_c = \frac{2\sigma_{ow}\cos\theta}{r} \quad (5)$$

Note that the capillary pressure is dependent on the interfacial tension for the two phases, the wettability (through  $\theta$ ), and the radius of the capillary ( $r$ ). It is inversely proportional to the size of the capillary and increases as the affinity of the wetting phase for the rock surface increases [5].

### 2.4.3 Viscous forces

The magnitude of the pressure drop that occurs when a fluid flows through a porous medium is a reflection of the viscous forces. With the simplifying assumptions of laminar flow and that the medium is made up of parallel capillary tubes, the pressure drop can be expressed by Poiseuille's law:

$$\Delta p = \frac{8\mu L v_{avg}}{r^2 g_c} \quad (6)$$

Where

$\Delta p$  is the pressure drop across the capillary tube [lbf/ft<sup>2</sup>]

$\mu$  is the viscosity of the fluid [lbm/(ft-sec)]

$L$  is the length of the capillary tube [ft]

$v_{avg}$  is the average velocity in the capillary tube [ft/sec]

$r$  is the capillary tube radius [ft]

$g_c$  is a conversion factor

### 2.4.4 Relationship of displacement forces

Now that the relevant forces have been defined we can take a brief look at how they interact with each other. The balance of the their magnitudes and directions influence how the fluids in the reservoir behaves. For a reservoir with two or more immiscible fluids the balance between gravity forces and capillary forces will yield the initial fluid distribution. This fact is utilized in reservoir simulation to find the initial state of the reservoir. For flow to occur in a porous medium the viscous forces must overcome the capillary forces [5]. Thus, the viscous and capillary forces govern the phase trapping and mobilization of fluids in a reservoir [5]. By consequence, the residual oil saturation and the microscopic displacement efficiency from section 2.1 are determined by the interaction of these forces. The trapping mechanism of fluids in reservoir rocks is

not completely understood, making a rigorous mathematical description impossible. It is known to depend on pore structure, fluid/rock interactions related to wettability, and fluid/fluid interactions reflected in IFT and sometimes in flow instabilities [5]. Numerous studies have shown that residual oil saturation is a function of a dimensionless group describing the ratio of viscous to capillary forces. The dimensionless group, called capillary number, is defined by equation (7).

$$N_{ca} = \frac{v\mu_w}{\sigma_{ow}} \quad (7)$$

Where

$N_{ca}$  is the capillary number

$v$  is interstitial velocity

$\mu_w$  is the viscosity of the displacing phase

$\sigma_{ow}$  is the interfacial tension for the displacing and displaced phase.

Higher capillary numbers correlate to lower residual water saturations. Experimental results show that for capillary numbers less than  $10^{-6}$  the residual oil saturation is relatively constant [10, 11]. As the capillary number in a typical waterflood is less than  $10^{-6}$ , measures must be taken to increase the capillary number if the residual oil saturation is to be reduced. From equation (7) we can see that this can be achieved by lowering IFT between the displaced and displacing phase or by increasing flow rate and/or viscosity of the displacing fluid. Polymers (for increased viscosity) and surfactants (for reduced IFT) are commonly added to the injection fluid to increase the capillary number.

## 2.5 Oil components

Crude oil consists of several distinct components of varying molecular weight. It has been observed that crude oil can alter the wettability of reservoir rocks. This is attributed to surface-active polar compounds in the oil, containing nitrogen, oxygen, and/or sulfur [12, 13, 8, 7]. The polar components, found in the resin and asphaltene fractions, possess both hydrophilic and oleophilic properties and collect at the interface between oil and water in the pores. If the water film breaks, or the components are given enough time to pass through it, they can adsorb onto the mineral surfaces of the rock, yielding a mixed or intermediate wetting [12, 14, 7]. The compounds containing oxygen are usually acidic, and include phenols and a wide range of carboxylic acids [8]. Among the sulfur compounds, sulfides and triophenes occur, with mercaptans and polysulfides in smaller amounts. The nitrogen compounds are generally basic or neutral and include carbazoles, pyridenes, amides, porphyrins, and quinolines [8]. Quinoline is often used to simulate basic polar components in adsorption studies [3, 15, 16, 17, 18].

## 2.6 Sandstones

Sandstones are formed when fragments, or clasts, of rock that have been weathered and eroded are deposited and subjected to burial by later deposition. The fragments are mostly made up of rock grains and mineral particles stemming from an igneous, metamorphic, or sedimentary rock formation. Depending on the geography of the area, the clastic material can come from sources nearby or be transported in suspension over long distances. Common depositional environments for sandstones include beaches, deserts, alluvial fans, deltas, and river channels. As deposition continues over long intervals of time the sediments are buried by overlying material, pressure and temperature increasing as the burial depth increases. Overburden pressure compresses the clastic material, expelling fluids and reducing the pore space between grains. At higher temperatures, dissolution and reformation of mineral grains take place within the rock in a process referred to as diagenesis. Silica ( $\text{SiO}_2$ ) and calcium carbonate ( $\text{CaCO}_3$ ) precipitate from solution and cement the individual rock grains together, resulting in a sedimentary rock.

An abundance of different minerals, rock fragments, compounds, and biogenic material can be present in a sandstone, quartz ( $\text{SiO}_2$ ) being the most abundant constituent. Because of the high content of silica, sandstones are often referred to as siliciclastic rocks in the literature. Also worth mentioning are feldspars and clays as they can greatly affect the properties of sandstones in a reservoir. The properties of porosity and permeability are primarily decided by the depositional environment through sorting and homogeneity of the clastic material, but are also correlated with burial depth. Well sorted (small deviation in grain size) sandstones are expected to have larger porosities relative to poorly sorted comparable sandstones. It will be shown in chapter 4 that clay minerals can alter porosity, permeability, wetting properties, and fluid distributions in a reservoir.

## 2.7 Clay minerals

Clay minerals are usually, but not necessarily, made up of sheet silicate materials, also referred to as phyllosilicates. The term “clay mineral” can also be applied to fine grained minerals “which impart plasticity to clay and which harden upon drying or firing” [19]. Silica, aluminum, water, iron, and magnesium constitute the most common building blocks, with potassium and sodium also commonly present in smaller amounts. Keep in mind that “clay” is an ambiguous term and the source of much confusion if not properly specified. When referring to clay as a property of particle size different disciplines use their own values, which can range from  $< 1 \mu\text{m}$  to  $< 5 \mu\text{m}$  [19]. It is well known that clay minerals can form particles that are larger than these values [20], and care should be taken when using a definition of clays based on particle size. The term is also used to describe formations, or strata of rock, which are comprised largely of clay minerals. Properties of some clay minerals commonly found in sandstone reservoirs can be found in table 1.

Table 1: Properties of some common clay minerals. Excerpt from [21].

Property	Kaolinite	Illite/mica	Montmorillonite	Chlorite
Structure	1:1	2:1	2:1	2:1:1
Particle size [micron]	5-0.5	Large sheets to 0.5	2-0.1	5-0.1
CEC [meq/100g]	3-15	10-40	80-150	10-40
Surface area BET [m <sup>2</sup> /g]	15-25	50-110	30-80	140

### 2.7.1 Structure and properties

The crystal structure of clay minerals is made up of thin layers of octahedral aluminum sheets (O) and tetrahedral silica sheets (T). Sketches of the sheets and their individual constituents are shown in figure 2. The octahedral and tetrahedral sheets are bound together in different ratios, such as 1:1 for kaolinite and 2:1 for illite. The ratio of tetrahedral to octahedral sheets is useful for classifying the clay minerals, and the different ways that these sheets are stacked and bound together give rise to different properties.

Kaolinite has one tetrahedral sheet bound to one octahedral sheet by shared oxygen atoms, and this combination is the fundamental unit of the mineral. Unlike other clay minerals, its units are not bound together by interlayer ions, but by hydrogen bonds between the oxygen in the tetrahedral sheet and the hydrogen from the OH-group in the octahedral sheet. Through of the additive power of these hydrogen bonds (which are individually weak) the units form crystals which can have a likeness to a stack of books or pseudo-hexagonal plates. An image of pseudo-hexagonal kaolinite plates is shown in figure 3. Because of the strong bonding between successive units, kaolinite does not swell. Kaolinite is encountered in many formations of varying age in the North Sea. Based on semi-quantitative estimates it occurs in intermediate to high concentrations in the middle Jurassic sediments of the Brent-group, as well as in Triassic sediments such as the Snorre field [4]. Pore-filling behavior is typical of kaolinite.

Illite is classified as a 2:1 clay, meaning that a single unit is made up of an octahedral sheet sandwiched between two tetrahedral sheets. Interlayer potassium (K<sup>+</sup>) bonds with the oxygen from the bottom tetrahedral sheet of the top unit, and its counterpart at the top of the bottom unit, forming an O-K-O bond. This bond is strong enough to prevent swelling [23]. Like kaolinite, illite is a common clay mineral in the North Sea, especially in the Rotliegend stratigraphic unit of Permian age. It is also found in high or intermediate concentrations in some formations of Triassic or Tertiary age, and in varying concentration in Jurassic formations [4]. Note that illite occurs only in small amounts for burial depths shallower than 3,5 km [4, 24]. Fibrous illite, as shown in figure 3 is known to bridge pores and pore throats, reducing permeability.

Chlorite is a 2:1 layer clay, consisting of a negatively charged T-O-T sandwich

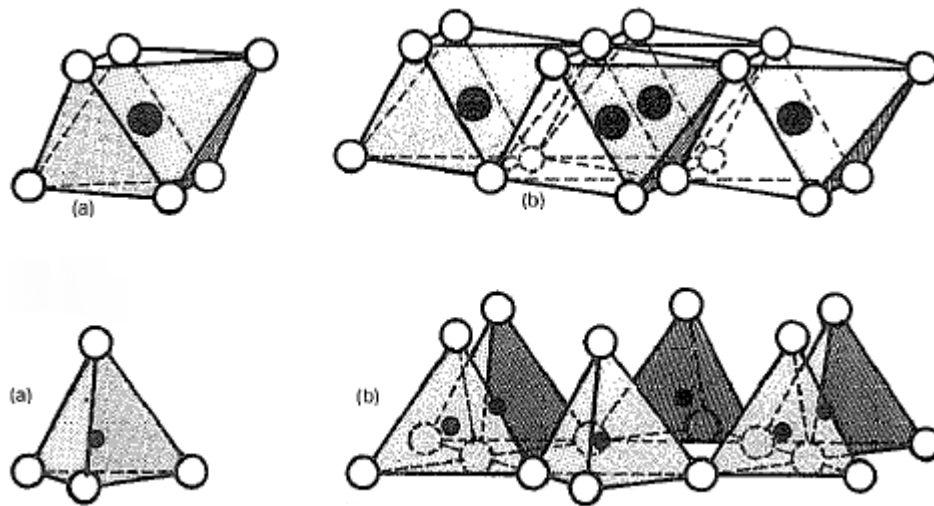


Figure 2: Diagrammatic sketches of octahedral (top) and tetrahedral (bottom) units and sheet structures. Modified from [21].

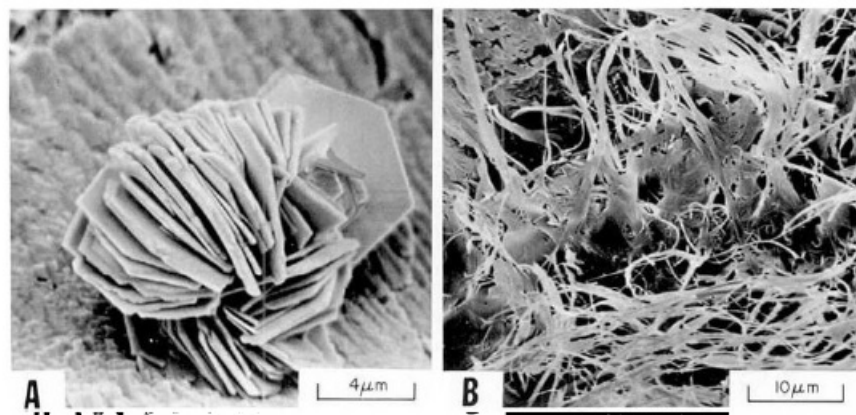


Figure 3: Clay mineral morphology. A: Pseudohexagonal kaolinite plates; B: Authigenic fibrous illite. Figure from [22].

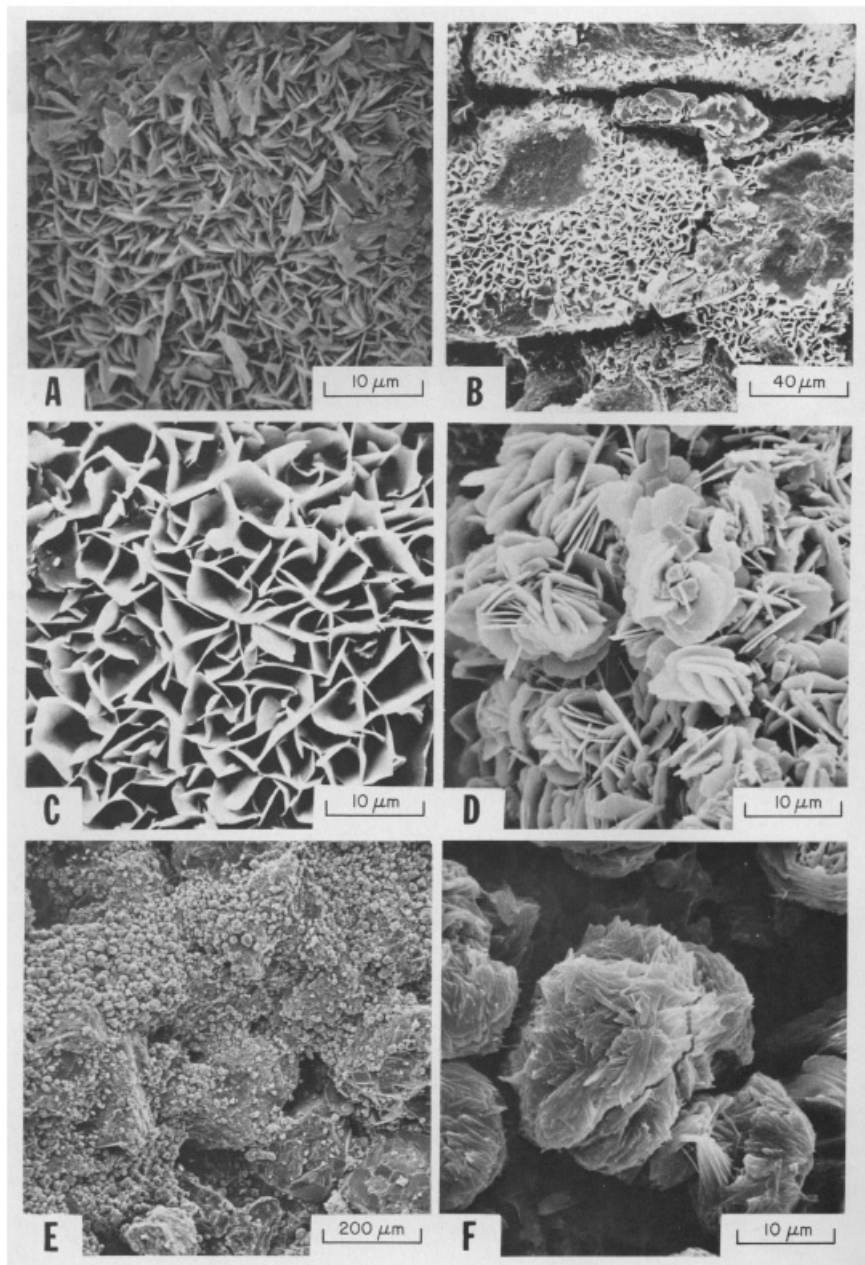


Figure 4: Chlorite growth habits. A: SEM-image of chlorite coating a sand grain; B: Chlorite honeycomb growth pattern coating sand grains. Dark spots outline points of contact with removed adjacent grains; C: Enlarged view of honeycomb growth pattern; D: Chlorite in the form of pore-filling rosettes; E: Low magnification view of cabbagehead chlorite coating sand grains; F: Magnified view of cabbagehead growth pattern. Figure from [22].



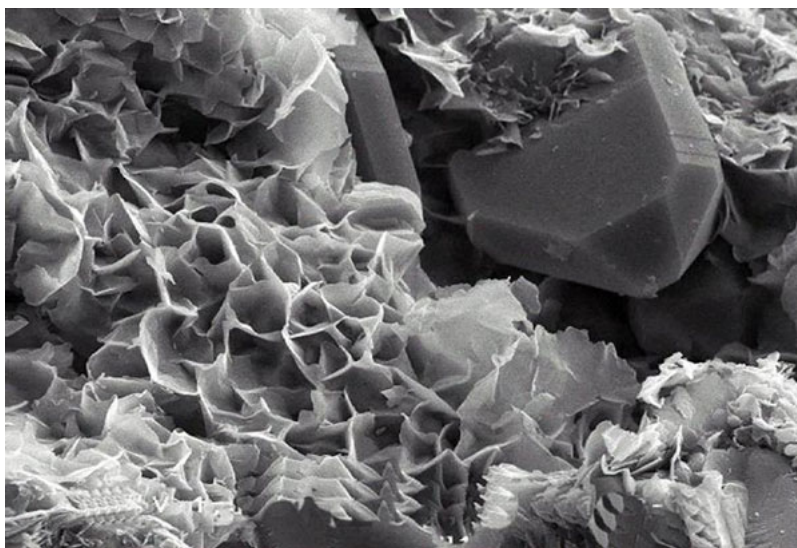


Figure 5: Montmorillonite honeycomb morphology. Figure from [23].

structure where the interlayer space is occupied by an additional brucite-like sheet. This hydroxide sheet is similar to an octahedral sheet, but positively charged, and sometimes referred to as a “brucite shee” because of its similarity to the mineral brucite ( $\text{Mg}(\text{OH})_2$ ). Comprised of cations ( $\text{Fe}^{2+}$ ,  $\text{Mg}^{2+}$ ) and hydroxyls (OH), the sheet binds one T-O-T layer to another [23]. According to Bjørlykke, chlorite is common but rarely abundant on the NCS [4]. It is found in intermediate and high concentrations in formations of Tertiary age in the North Sea, such as the Balder, Heimdal, and Sleipner fields [4]. Chlorite is a pore-lining material, and deposits in reservoirs grow inward from the pore walls. It is the most variable in form among the authigenic clays and can exhibit several different growth habits. Some images of chlorite are shown in figure 4.

Montmorillonite is a 2:1 clay, and is the most common mineral of the smectite family. Like illite, it consists of an octahedral sheet sandwiched by two tetrahedral sheets. It has a varying content of water, giving it a large potential for swelling. Due to the fact that ionic substitutions mainly occur in the central octahedral sheet, the cations that balance the negative charge are unable to get close enough to the charge sites to completely balance them. This means that the structure retains some of its ionic character, making adsorption of polar components, namely water, possible between the unit layers. When fully hydrated, montmorillonite expands to just single unit layers when dispersed in water, giving it a very large surface area. This complete expansion is made possible when sodium is the exchangeable cation. A divalent cation such as calcium will adsorb to charge sites on two sheets at once, binding the sheets together. Montmorillonite is the major clay mineral in “bentonite”, a common additive in drilling fluids, where it is used to increase viscosity. Natural bentonite occurs

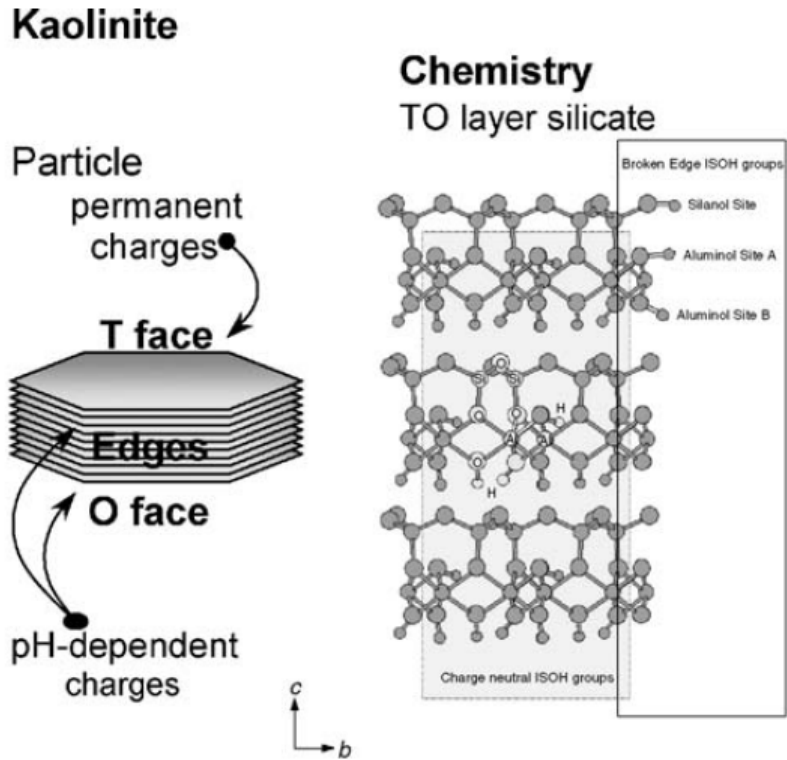


Figure 6: Charge sites on kaolinite clay mineral particle. Figure from [25].

in the calcium form, with the notable exception of the Wyoming variety. It is often chemically treated with sodium carbonate to partially convert it to the sodium form, as this is the preferred form for drilling fluid application. Montmorillonite, like other smectites and chlorite, is known to coat pores. Unlike chlorite however, the coating is found to be smooth and regular. An image of montmorillonite forming a honeycomb-like structure is shown in figure 5.

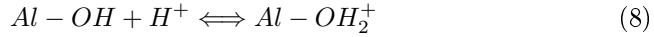
### 2.7.2 CEC and surface reactivity

Clay minerals are characterized as cation exchange materials. Charge imbalances, either in the tetrahedral sheet, the octahedral sheet, or on the edges charge the surfaces of the clay. These structural imbalances arise from isomorphous substitution in the lattice structure, broken bonds at the edges and surfaces, and dissociation of hydroxyl groups. In the tetrahedral sheet, substitution of  $\text{Si}^{4+}$  in favor of ions such as  $\text{Al}^{3+}$  or other ions of a lesser valence yields a negative charge. Likewise, substitutions of  $\text{Al}^{3+}$  in favor of  $\text{Mg}^{2+}$  may take place in the octahedral sheet. Isomorphous substitution creates a net negative charge which is independent of pH. In order to balance these charges, cations

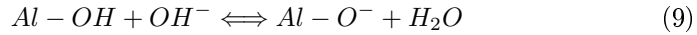
from the surrounding fluid medium are adsorbed onto the clay. These adsorbed cations can be exchanged for others, which may be of the same type or different cations. Cations have varying affinities for the clay surface, this hierarchy is generally believed to be, in order of highest to lowest affinity at room temperature:  $H^+ \geq Ba^{2+} \geq Sr^{2+} \geq Ca^{2+} \geq Mg^{2+} \geq K^+ \geq Na^+ \geq Li^+$  [21]. This relation states that calcium would displace more sodium ions than the other way around at equal concentrations. Which type of cations that are adsorbed also depends on the concentration of the ion. Thus, for a higher concentration of sodium relative to calcium, the number of adsorbed sodium ions may be higher than the number of adsorbed calcium ions. Cation exchange capacity is usually determined by measuring the adsorption of methylene blue, a cationic dye, and is reported as milliequivalents of dye adsorbed per 100 grams of dry clay. Even though the CEC is a characteristic of the clay mineral, we will see in chapter 4 that it is indeed variable.

In addition to the permanent negative charge from lattice substitutions, pH dependent charge sites may also exist on the clay particles. In an acidic environment exposed silanol or aluminol groups on broken edges and hydroxyl-terminated planes (O-faces) are protonated [25, 21], giving rise to positive charges as shown in equation (8) below. Conversely, under alkaline conditions the charges will be negative [21, 25], due to dissociation of the hydroxyl groups when contacted by  $OH^-$  as shown in equations (9) and (10). The location of permanent and pH variable charge sites are shown in figure 6.

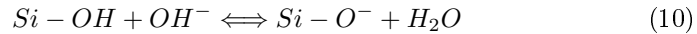
Protonation of aluminol in acidic environment:



Dissociation of aluminol hydroxyl group in alkaline environment:



Dissociation of silanol hydroxyl group in alkaline environment:



### 2.7.3 Origin

It was mentioned in section 2.6 that the clasts that form sandstones under compaction and burial can contain mineral particles. Such particles may be clay minerals or precursors to clay minerals, for example feldspars. Detrital clays refer to clay minerals which originated outside the rock they currently reside in. When the clay minerals are transported as dispersed matrix, sand-sized floccules, or sand- to cobble-sized mud or shale, and are deposited in a basin, they are classified as allogenic, or detrital clays [22]. The same is true if the clay is introduced after deposition as a result of infiltration or bioturbation, meaning that the sediment has been disturbed by animals or plants [22]. In contrast, authigenic clays are formed in-situ, by direct precipitation from formation water, or by diagenesis/reformation.

There exists several criteria which can be used to differentiate between detrital and authigenic clay minerals, the most obvious being the delicacy of the morphology. As an example, illite and mixed illite/smectite can develop a delicate fibrous texture, with spines or thread-like projections up to 30  $\mu m$  long [22], precluding extensive transport. Another clue to an authigenic origin are clays which line the pore walls except at the points of contact between grains, indicating that the coating was deposited after compaction and cementation. On the other hand, a high clay content in the matrix of the rock, and clay particles with rounded irregular edges are indications of an allogenic origin, as is an irregular size distribution. Authigenic clays tend to have well-formed crystals with sharp, easily recognizable edges and a more uniform size distribution owing to precipitation from pore water in-situ. Detrital clay can also be polymineralic, meaning that it is mixed with other minerals, and may contain silt or organic material. Sometimes it can be difficult to differentiate between authigenic clays and neoformed detrital clays which have dissolved and reprecipitated, as they have an appearance somewhere between detrital and authigenic. Clays are not limited to the rock matrix and pore space, but may also exist as layers of shale interstratified with the reservoir sand formation.

Detrital clay content can be an important indicator of depositional processes and environment. In addition, the type and origin of clay can have important effects on petrophysical properties, so interpretation of their origin could give valuable insights into their behavior in the pore-system and pertaining to their interaction with pore fluids.

#### 2.7.4 Diagenesis

During burial clay minerals and other minerals and components can be altered by chemical processes in the pore space. These reactions are responsible for the formation of authigenic clays, precipitation of quartz cement, quartz overgrowths, and calcium carbonate among others. At temperatures above 60°C smectite clay reacts with K-feldspar to form illite [26]. This origin of illite is abundant in Permian and Triassic reservoirs on the NCS [4]. Illite also forms from kaolinite and K-feldspar at temperatures exceeding 100°C [27, 28]. An increase in illitization of kaolinite is observed below 3,7 to 3,8 km burial depth in several oil fields [4, 24, 29, 28]. Flushing by fresh water during early burial or tectonic uplift is known to dissolve feldspars and precipitate diagenetic kaolinite. The degree of flushing is controlled by depositional environment, continuity of sandstone beds, and climate [4]. This reaction is often observed to take place in Jurassic formations, and explains the abundance of kaolinite in these reservoirs. Authigenic chlorite may replace kaolinite or smectite provided that the supply of iron and magnesium is sufficient. Occurrence of chlorite is commonly associated with biotite and other ferro-magnesium minerals [4]. The chemical composition of clay minerals exhibit temperature dependence, as authigenic clays become unstable with increasing burial. In a process called “Ostwald ripening” the clay adjusts to the new conditions by dissolution and re-precipitation. [4]. Smaller grains are dissolved and re-precipitate on the more stable larger particles, record-

ing chemical adjustments to temperature and porewater composition over time analogous to tree rings. Porosity, permeability, wetting properties, and water saturations are all affected by diagenetic reactions, often in such a way that reservoir quality is reduced. A more extensive description of these processes and their effects will be given in chapter 4.

## 2.8 Water injection

Waterflooding is the most widely used secondary recovery process in petroleum engineering, to the extent that secondary recovery is now almost synonymous with waterflooding. Its purpose is to displace oil from a reservoir and to provide pressure maintenance as the reservoir is depleted of oil. Water is inexpensive and readily available, and therefore favorable as an injection fluid. Some of the most important parameters [5] that decide waterflood efficiency are listed below.

- Properties of injected fluids (density, viscosity, relative permeability, ionic composition etc.)
- Properties of displaced fluids
- Geometry of injection and production well patterns
- Rock properties and geology
- Clay content, oil composition, composition of formation water [3].

The mobility ratio between water and oil defined in equation 11 below is a key parameter for displacement efficiency, with recovery increasing as mobility ratio decreases [30, 5]. This definition assumes piston-like flow with only water flowing behind the flood front, and only oil flowing ahead of the front.

$$M = \left(\frac{k_{rw}}{\mu_w}\right)_{S_{or}} \left(\frac{\mu_o}{k_{ro}}\right)_{S_{iw}} \quad (11)$$

Where

$M$  is the mobility ratio

$k_{rw}$  is the relative permeability to water

$\mu_w$  is the water viscosity

$\mu_o$  is the oil viscosity

$k_{ro}$  is the relative permeability to oil

The subscripts  $S_{or}$  and  $S_{iw}$  indicate that the relative permeabilities are measured at residual oil saturation and interstitial (immobile) water saturation, respectively [5]. At mobility ratios above unity instabilities in the flow cause a phenomenon known as viscous fingering, leading to early breakthrough of water and reduced sweep efficiency. Because of this, mobility ratios larger than unity

are referred to as unfavorable, while ratios smaller than unity are referred to as favorable. As mentioned in section 2.4.4, polymers can be added to the injected water to increase viscosity, yielding a more favorable mobility ratio. The effects of clay, oil composition, composition of formation water, and composition of injected water will be discussed in chapter 3.

### 3 “Low salinity injection” and “smart water”

The first known observation of increased oil recovery attributable to injection of low salinity water comes from a study by John C. Martin in 1959. Martin identified the clay minerals present in the rock as the cause for the improved recovery of a high viscosity crude and tried to derive a plausible mechanism for the effect. By his own admission the results of the analysis “should be considered as being somewhat speculative until the assumptions are verified.” Nevertheless, he concluded that “fresh water may be a more desirable injection fluid than brine in some highly permeable reservoirs containing high viscosity crudes.” [31]. Another important study from the early stage of research was put forward by George G. Bernard in 1967. Bernard flooded both synthetic and natural cores with water of varying salinity in order to increase the oil recovery, in this case simulated by Soltrol recovery. He found that the effect only became apparent when salinity was reduced to less than 1 weight% of NaCl. The first mechanism he proposed hypothesized that swelling of the clay reduced the pore volume of the rock, thereby expelling fluid. He noted in his discussion that this effect alone could probably not produce the observed effect. In his second mechanism proposal he attributed the increased recovery to the water dispersing the clay particles and transporting them in suspension. He further supposed that the suspended clay plugged some of the established paths of flow, and that as a result new paths were established and flooded out, leading to a higher recovery [32].

In later years there has been a wealth of research conducted on low salinity water injection, with several authors of different affiliations publishing papers on the subject. Composition of injection brine has been shown by numerous studies to have an effect on oil recovery [33, 3, 34, 35, 36, 37]. Note that different authors use different terms when referring to the increased recovery after low saline water injection. Some opt for “low salinity effect”, while others use trademarked names, one example being LoSal<sup>TM</sup> [33]. It appears that composition of the injected water is a more important parameter than its salinity [17, 18, 38, 35], and this thesis will therefore adopt the term “smart water” or “smart water effect” from this point onwards.

#### 3.1 Conditions for “smart water” effect

From the knowledge accumulated over years of research there appears to be at least three necessary conditions for observing a “smart water effect”:

1. Clay minerals must be present [37].

2. Polar components must be present in the crude oil [37, 39].
3. The formation water must contain active cations such as  $\text{Ca}^{2+}$  and  $\text{Mg}^{2+}$  [38, 35].

## 3.2 Proposed mechanisms

The complexity of the interactions between crude oil, brine, rock, and injected fluid has led to several different explanations for the observed effect of water composition on oil recovery. Although there seems to be a general agreement that certain conditions need to be fulfilled for the effect to occur, and that the effect is probably caused by a wettability alteration towards more water-wet, the mechanisms that explain it are diverse. In the following sections a brief overview of some of the explanations will be given. More comprehensive reviews are given by a PhD thesis by RezaiDoust [14].

### 3.2.1 Migration of fines

This mechanism, put forward by Tang and Morrow in 1999, hinges on the existence of potentially mobile fine particles on the rock surface. These particles adsorb polar components from the oil, thus obtaining a mixed wetting. During low salinity injections in Berea sandstone cores, the researchers observed fines, mostly kaolinite, in the effluent. A permanent reduction in permeability was also usually observed in connection with this production of fines. The researchers proposed that the particles were stripped from the pore walls during flooding with low saline water and that they were subsequently carried away at the interface between the oil bank and the injected water [37]. The mobilization of these mixed-wet particles was believed by the researchers to reduce residual oil saturation, increasing recovery. As for the stripping mechanism, they linked it to the expansion of the electrical double layer in the water phase between the fine particles when water of low ionic strength was injected [37]. When the fine clay in the cores were stabilized by firing at  $800^{\circ}\text{C}$ , they exhibited no sensitivity to salinity, supporting this hypothesis [37]. Skauge et al., 2008 expanded on this idea and put forth an alternate explanation for how mobilization of fines could yield increased recovery [14]. They proposed that mobilized fines were able to block pore throats, diverting the water into unswept pores, thereby increasing the sweep efficiency [14].

### 3.2.2 pH related to alkaline flooding

Increases in pH of 1-3 units are commonly observed in waterflooding tests. McGuire et al, 2005 [40] noted the similarity between the increased recovery when injecting low salinity brine and the increased recovery during alkaline flooding. In-situ generation of surfactants, reducing IFT between oil and water, was proposed as the reason for the improved recovery. The acidic components in the crude was believed to be the origin of these surfactants. Divalent cations such as  $\text{Ca}^{2+}$  and  $\text{Mg}^{2+}$  in high concentrations will precipitate the surfactants,

reducing their effect on IFT. The lower concentration of these cations in the low salinity brine reduced this precipitation, facilitating IFT reduction and higher microscopic displacement efficiency. The pH increase could be explained by CEC activity (see equation (12)) and dissolution of carbonate cement [14]. In contradiction of this study, Lager et al. found no direct correlation between the acid number of the crude and the amount of oil recovered, and pH induced IFT reduction was seen as an effect rather than a cause [33]. Increases in oil recovery have been observed by others with little or no increase in pH [39, 33].

### 3.2.3 Multi component ion exchange (MIE)

Put forward by Lager et. al in 2006, this theory is based on the assumption of competition for charge sites on the rock between the ions in the brine. Polar components can adsorb onto the clay directly by cation exchange, or by forming an organo-metallic complex which is adsorbed onto the clay by a multivalent cation bridge [38]. Injection of brine with low concentration of  $\text{Ca}^{2+}$  and  $\text{Mg}^{2+}$  causes multi-component ion exchange (MIE) to take place between adsorbed polar components, cations in the in-situ brine, and clay mineral surfaces. This disturbs the ionic equilibrium, and divalent cations from the low salinity brine exchange with cationic organic complexes or with bases [14]. As a result of this, organo-metallic complexes and organic polar compounds are removed from the clay, increasing water wetness. Expansion of the electrical double layer was also suggested to play a part in the improved recovery. It was noted that removal of divalent cations from the formation water extinguished the salinity sensitivity of oil recovery. During a later field test in Alaska, a strong decrease in concentration of  $\text{Mg}^{2+}$  and a smaller decrease in  $\text{Ca}^{2+}$  concentration in the produced water was measured, supporting the importance of these divalent cations [34]. For the MIE mechanism to hold true, there must be a low concentration of calcium and magnesium ions in the injected water to replace those adsorbed on the clay surface, causing desorption of polar compounds. Contrary to this, successful low salinity floods have been carried out with no divalent cations in the injected water [35].

### 3.2.4 Expansion of the ionic electrical double layer

In 2009, Ligthelm et al. suggested a mechanism based on DLVO theory and expansion of the electrical double layer. It was proposed that by lowering the ionic strength of the brine reduced the screening potential of the cations. This leads to expansion of the electrical diffuse double layers that surround the clay and oil particles, and increase the absolute level of the electrostatic potential. In turn, this increases the electrical repulsive forces between the clay and the oil. They further wrote that once the repulsive forces exceed the binding forces of the multivalent cation bridges, the oil may be desorbed from the clay surface [35]. This desorption leads to a wettability alteration in the direction of more water-wet as predicted by wetting theory. Also worth noting is that the study warned against too low ionic strengths, as the increased repulsion was believed



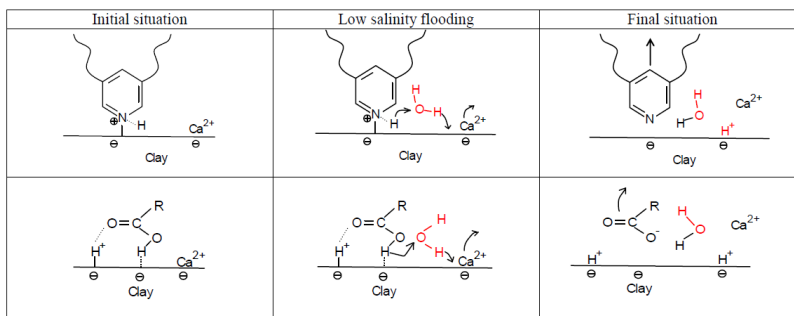


Figure 7: “Smart water” desorption mechanism. Desorption of basic (top) and acidic (bottom) polar components. Figure from [3].

to lead to deflocculation of the clay, stripping it from the pore walls. This warning of formation damage by fines migration was a reference to the studies of Tang and Morrow, 1999a which was mentioned in section 3.2.1, and Zhang et al, 2006.

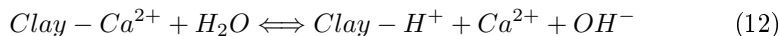
### 3.2.5 Desorption by pH increase

Suggested by Austad et. al. in 2010 [3], this mechanisms forms the starting point for this thesis, and most of the content in the following section was acquired from their paper. None of the mechanisms described in the preceding sections have gained universal acceptance as the sole cause for the “smart water effect”. Based on their own experimental observations, the research group set out to explain their observations by a new chemical model. The wettability alteration of the reservoir rock was suggested to be a result of desorption of polar compounds by means of acid-base reactions at the interface between the clay and water. It was assumed that the following factors would play a major role in the performed experiments:

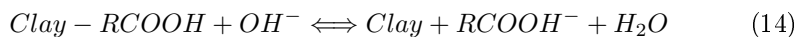
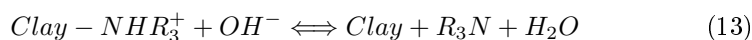
- Clay properties/type and the amount present in the rock.
- Polar components in the crude oil, both basic and acidic.
- The initial formation brine composition and pH.
- The EOR effect of “smart water” flooding is caused by improved water wetness of the clay minerals present in the rock.

As discussed in section 2.5, organic material from the crude, both acidic and basic, is adsorbed onto the clay minerals together with cations such as  $\text{Ca}^{2+}$ . A chemical equilibrium is then established, obeying reservoir conditions such as temperature, pressure, pH etc. When a fluid with a lower ionic strength, and a particular composition is injected as a secondary or tertiary flood this equilibrium between brine and rock is disturbed, leading to a net desorption

of cations, especially  $\text{Ca}^{2+}$ . This loss of positive charges on the clay surface must be compensated for. Protons ( $\text{H}^+$  ions) from the water adjacent to the clay adsorb onto the clay, balancing the charges. The clay acts as a cation exchanger, substituting  $\text{Ca}^{2+}$  with  $\text{H}^+$ . When the bonds of the water molecules are broken, and  $\text{H}^+$  is adsorbed onto the clay, free hydroxyl ions increase the pH in the region close to the clay. This reaction is given by equation (12).



As shown in the following equations, using  $\text{Ca}^{2+}$  as an example, the hydroxyl reacts with the bound polar components on the clay, facilitating their desorption:



The suggested mechanism for the desorption process of acidic and basic materials is illustrated in figure 7.

## 4 Results and discussion

### 4.1 Effect of clay minerals on reservoir properties

The way that clay minerals influence reservoir properties have been referred to in earlier chapters, but it has not been thoroughly explained. This section will be more specific in that regard, discussing effects, benefits, and detrimental results of clay content in reservoir rocks. It is well known that clay content can affect reservoir quality in a number of ways. Permeability reduction, increased irreducible water content, wettability alterations, and lowered effective porosity are important examples of this. However, the effects are not always negative.

#### 4.1.1 Porosity

Clay minerals can affect porosity in a few different ways, depending on clay type, origin, and distribution in the rock. Detrital clay in the form of interstratified laminae of shales will reduce the bulk porosity of a reservoir volume, and in dispersed form it can fill pore space. Partial or complete dissolution of feldspar, a common reaction during diagenesis, creates molds of secondary porosity. However, this only serves to redistribute porosity as the dissolved material is mostly precipitated as kaolinite and quartz nearby. The molds, or secondary porosity, created by the dissolution reaction may not be well enough connected to add to the effective porosity of the rock. The precipitation products, quartz and kaolinite, take up space in the pores, and kaolinite deposits have associated microporosity which may not contribute to hydrocarbon storage [42, 24]. As an overall result of the reaction, secondary porosity and microporosity is created at the expense of effective porosity, reducing reservoir quality [28].

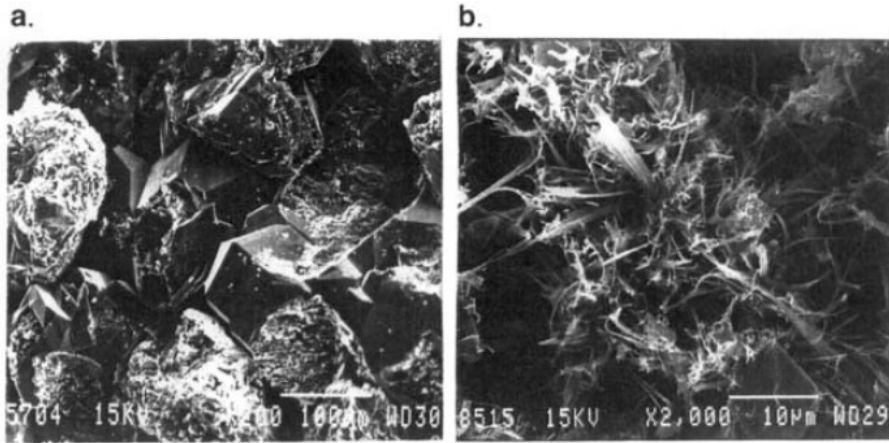
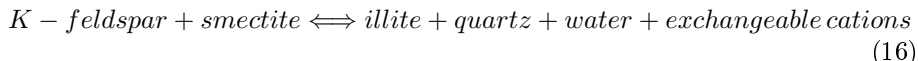


Figure 8: Electron micrographs of diagenetic quartz cement (a) and authigenic illite (b). Note the fibrous texture of the illite which gives it high microporosity, significantly decreasing permeability. Figure from [41].

Microporosity can have strong negative effects on reservoir quality. Nadeau and Hurst, 1991, used an image analysis system in conjunction with back-scattered electron microscopy to study microporosity in sandstone samples from North Sea formations. Microporosity was defined as “porosity encompassed by, and directly associated with, clay minerals”. They found that authigenic clays possess significantly higher microporosities than clay-rich detrital clasts in sandstones [42]. Authigenic kaolinite was found to have an average microporosity of 43%, with measurements varying significantly for different textures. Vermicular (worm like) crystals had microporosities in the range of 45-50%, while blocky crystals had lower values, in the range of 15-30% [42]. Pore lining/grain coating chlorite was also studied, and was found to have an average value of 51% with smaller deviations from the mean relative to kaolinite. Diagenetic illite proved hard to characterize due to collapse of their delicate structures during air-drying of the cores. The data from BSE image analysis showed an average microporosity of 63% for illite, but the researchers theorized that the real value should be higher [42]. In a later study by the same researchers the microporosity of fibrous illite was estimated from SEM images to be 90% [20]. They calculated that less than 2% by weight of diagenetic illite can reduce the effective porosity of a sandstone with 25% total porosity to approximately 0%. Illitization of kaolinite is a major factor in porosity reduction for reservoirs at depths greater than 3.5-4 km on the NSC, but the kinetics of the reaction are not well understood [24, 29, 28]. Whether illitization was a rapid process only dependent on temperature or a slower process dependent on both temperature and time has been a subject for debate [28]. The second alternative is an analogue to the thermal alteration of organic matter where thermal maturity is the limiting factor [28].

It has been theorized in a number of publications that the presence of hydrocarbons in the pores could inhibit illitization [41]. However, study of cores and modeling of hydrocarbon accumulation done by Ehrenberg and Nadeau in 1989 contradict this theory. No inhibition or indication thereof was found for hydrocarbon bearing reservoir rock, and the researchers proposed that 20-30% water saturation was sufficient for short-range diffusive transport of the reaction material [28]. Frequency distributions of porosity for water and HC bearing zones from the NCS have also failed to show any indication of porosity preservation by hydrocarbons [41]. In his 2011 paper, Nadeau states that misconceptions about illitization inhibition by HC, as well as concepts proposing porosity *increase* with increasing depth and temperature, have been detrimental to understanding the process of porosity loss by mineral diagenesis [43].

Studies from the NCS have shown that after mechanical compaction, quartz cementation is the most important mechanism for porosity loss in deeply buried sandstones [41, 24, 29]. Petrographic studies of dissolution textures from the NCS have shown that quartz dissolution primarily takes place at mica/quartz and illite/quartz interfaces [41]. This dissolution process provides silica for quartz cement precipitation, leading to the observed porosity loss. The overall rate of the process is strongly controlled by the precipitation step, which is exponentially related to temperature [41, 44]. The exponential increase in cementational porosity loss at temperatures over 120 °C is a major contributor to reservoir overpressure development and seal failure in low permeability shales [43]. An example of how quartz cement precipitates and reduces porosity is shown in figure 8a. The required silica for precipitation of quartz cement may also stem from illitization of kaolinite, as shown by equation (15), or from illitization of smectite, as shown by equation (16). Kaolinite precursors are more common in the North Sea, while smectite precursors dominate on the US Gulf Coast [27, 28, 43]. The onset of the reaction is thought to occur at about 60°C in the absence of carbonate minerals, which may increase the stability of the reactants to approximately 80°C [26, 43].



Chlorite is interesting because it may exhibit both positive and negative effects on reservoir quality. Its growth habits include grain coating, or pore lining, where the chlorite grows inward from the pore wall. This will reduce the pore space by a relatively small amount, but will have more profound effects on water saturation (through microporosity) and permeability. These negative effects can become significant for thick coatings over 4  $\mu m$  [46]. The primary effect on porosity for chlorite derives from its inhibition of diagenetic quartz cement formation, preserving anomalously high porosities with burial. [46, 45]. A study of five Lower to Middle Jurassic sandstone reservoirs from the NCS found clear indications of deep porosity preservation by authigenic chlorite [45]. Maximum

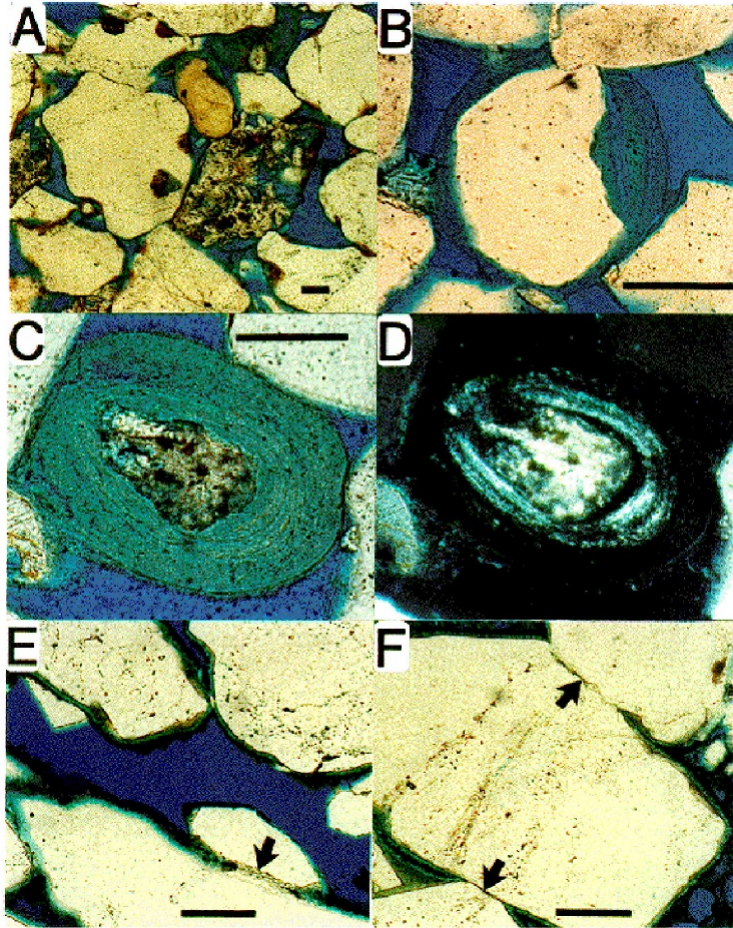


Figure 9: Photomicrographs of sandstones from Tilje formation. Scale bar = 0.1 mm for all images. A: Chlorite coatings, shown in brown, have been effective in inhibiting quartz cement growth. Thicker coating in indentations suggests a significant detrital component, present as at least a partial coating of iron-rich clay during deposition [45]; B: Quartz grain surrounded by a coating of concentrically laminated chlorite; C: Chlorite-rich sedimentary grain developed around a rock fragment. The outermost 4-6  $\mu\text{m}$  are radially oriented with the rest of the coating exhibiting concentric lamination [45]; D: Same view as C with polarizing filters crossed. Varying color of layers represents ratio of chlorite (dark) and illite (bright) [45]; E: Chlorite coating detrital quartz grains but not surfaces of quartz cement. Thin or absent coating at points of contact between grains and overgrowths [45]; F: Note the absence of coating at points of contact between grains. This is a common indication of authigenic origin [22, 45]. Figure from [45].

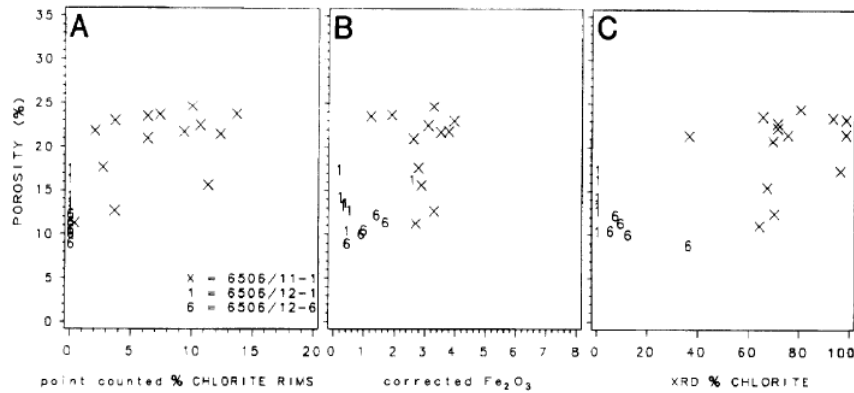


Figure 10: Helium-measured porosity of Tofte formation sandstones vs. indices of chlorite content for three different wells. A: Point counted % chlorite rims; B: Bulk-rock iron content minus iron contained in siderite and pyrite; C: % chlorite in clay fraction. Figure from [45].

porosities were found to be 10-15% higher than what would be expected from regional porosity/depth trends [45]. It has commonly been assumed that when chlorite coats detrital quartz grains, the quartz surfaces are isolated from the pore water, preventing nucleation of diagenetic quartz [45]. The Smørbukk field exhibits such anomalous zones, especially in the Tilje formation which contains over 50% of the in-place liquid reserves [45]. Images of chlorite coatings on samples from the Tilje formation are shown in figure 9. High chlorite content and preserved porosity is also evident in the core from well 6506/11-1 in the Tofte formation of the Smørbukk field [45]. Two neighbouring wells have also been cored, but show little chlorite and lower porosities [45]. The relation between porosity and chlorite content for these three wells are plotted in figure 10. It was mentioned in section 2.7.4 that chlorite can form from kaolinite during diagenesis provided that sources of magnesium and iron were present. Most of the chlorite in Jurassic sandstones seem to have been formed by this reaction [4]. Presence of mafic volcanic clasts, iron-rich river discharge, as well as dissolution of iron-rich smectite precursors may provide these components [4, 45, 46]. Examples of higher than expected porosity in chlorite rich sandstones can also be found in well cores from the Veslefrikk field, with the Intra-Dunlin sandstone unit being of special interest because of its high reserve content [45].

#### 4.1.2 Permeability

If clay minerals can be said to be a major factor in porosity reduction, it is obvious that they can influence permeability due to the link between the two. In fact, the detrimental effects on permeability are even more pronounced. Authigenic kaolinite which precipitates in the pore space tends to block pore throats,

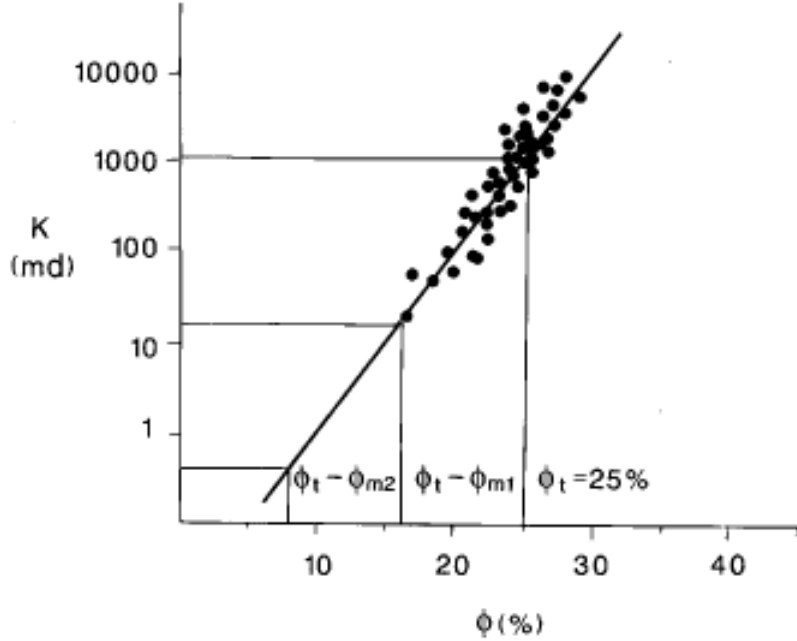
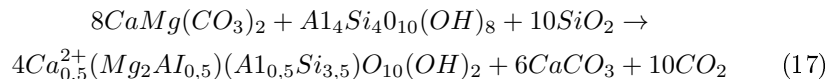


Figure 11: Porosity/permeability crossplot for typical North Sea sandstones.  $\phi_t$  represents total porosity while  $\phi_t - \phi_{m1}$  and  $\phi_t - \phi_{m2}$  represent estimates of effective porosity, where the subscript “m” denotes microporosity.  $m_1 = 90\%$  and  $m_2 = 95\%$ . Figure from [20].

reducing permeability if it is present in significant amounts. Extensive chlorite rims can reduce permeability, increase resistivity by increased water saturation, and change capillary pressure functions [46]. This is evident in core floods from the Åsgard field, where HCl was used to remove chlorite from the cores in order to study its effect on reservoir quality. Initial porosity of the two cores were approximately 0,24 and 0,25. This increased to about 0,27 and 0,28, respectively by HCl flushing [46]. Initial permeabilities were approximately 20 and 16 mD, and increased to ca. 43 and 44 md, respectively [46]. Given the fact that chlorite can inhibit growth of quartz cement, which is a significant factor in permeability decrease for deeply buried reservoirs, the contribution of chlorite is complex and cannot be easily quantified. Although the chlorite-effect can be considerable, literature study confirms that it is not nearly as dramatic as the permeability decrease observed for authigenic illite and smectite [4, 41, 43, 47, 20, 28]. Authigenic illite and smectite can exhibit delicate fibrous morphologies with significant microporosity between the clay particles. They commonly occur together as interstratified illite/smectite in different ratios and

with varying degrees of ordering [26, 48, 22]. The fibrous morphology with associated microporosity which was mentioned in section 4.1.1 can span the width of pores and pore throats, creating bridges of clay particles with tightly bound water in between. This phenomenon greatly disturbs flow in the pore system with the effect of severely reduced permeability. In a study by Nadeau and Hurst from 1995 the researchers calculated the effective porosity and the associated permeability decrease stemming from microporosity and presented it in the form of a cross plot. This cross plot is shown in figure 11. The calculations were based on less than 2 wt% of diagenetic illite. From the plot it can be seen that when effective porosity (correcting for microporosity) is used to estimate permeability, severe reductions are evident. For 90% microporosity, which is the value the researchers estimated from BSE images, permeability decreases by almost two orders of magnitude. With a microporosity value of 95%, which doesn't seem wholly unreasonable, the permeability has decreased by over three orders of magnitude, effectively sealing the reservoir. In another, experimental study [47], a smectite was hydrothermally grown from dolomite and kaolinite in a synthetic sand at 175-200°C for 19 to 45 days. The reaction is described by equation (17) which uses the idealized chemical formulae and a generalized half unit cell smectite formula [47].



The reaction is dominated by dolomite dissolution which provides Mg for smectite, Ca and  $CO_3$  for calcite, and  $CO_2$ . Kaolinite provides the Al and some of the Si needed for smectite formation with the rest of the Si (about 70%) being provided by quartz [47]. The synthetic smectite was determined to be saponite, and CEC calculations indicated that the maximum content formed was in the range of 2-3 wt% [47]. Although relatively little saponite was formed, brine permeability was reduced by up to 98%. A relation between brine permeability and process conditions is given in figure 13. When the sample was air-dried the clay morphology was destroyed by surface tension and collapsed into a pore lining form, this is shown in figure 12E and F. This process is irreversible and air-dried samples resaturated with brine exhibit increased permeability as seen in figure 13. Because of this collapse air-dried reservoir cores may not represent actual subsurface conditions, and critical-point drying is suggested as an alternative [47].

It seems plausible that the reaction shown in equation (17), as well as the reaction paths shown in equations (15) and (16) could have implications for thermal EOR processes. During cyclic steam injection (CSI) the injection and subsequent "soaking" processes could last for days or even weeks, and a well may undergo several of these cycles [5]. The temperature in the reservoir during CSI reaches 200-300°C [49] which is more than enough for the aforementioned reactions to occur. Seeing as the oil extracted in processes such as cyclic steam injection and steam assisted gravity drainage are very viscous, permeability



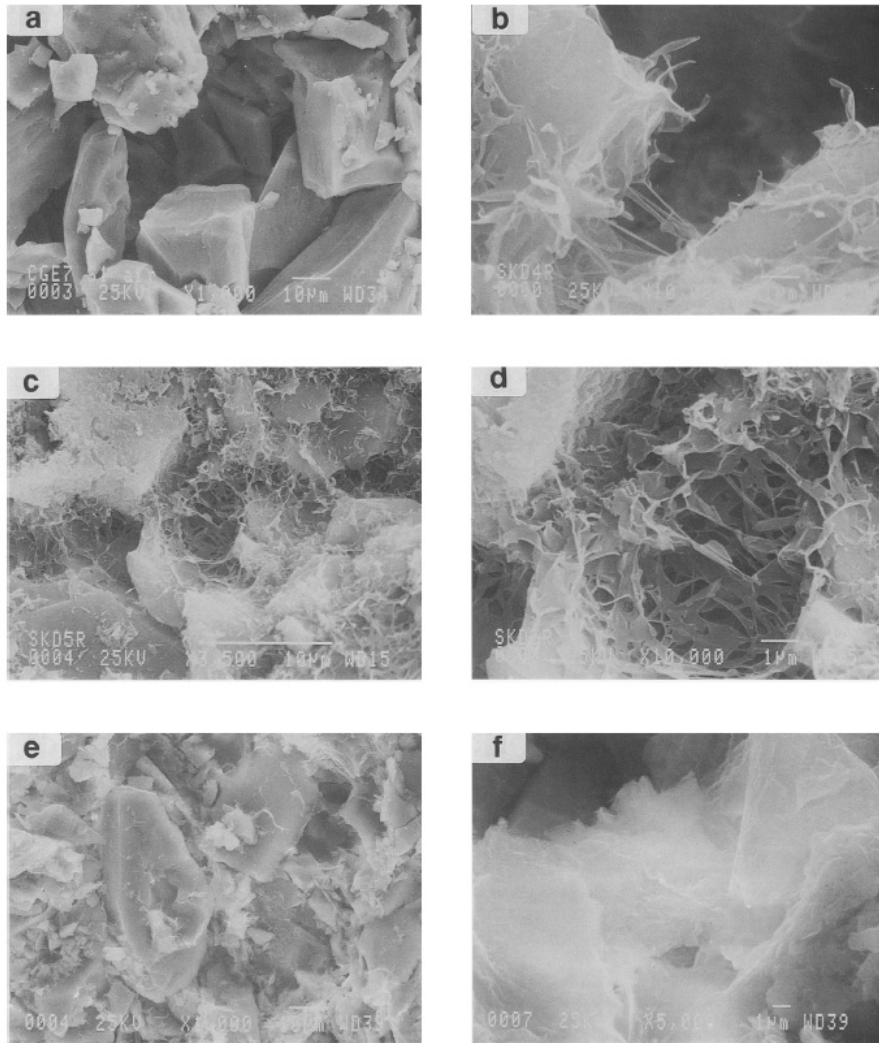


Figure 12: SEM images of synthetic smectite growth. A: Control sample (100% quartz); B: Early stage growth. Extremely thin individual clay particles; C and D: Microporous and delicate pore-bridging morphology covering most of the available pore space; E and F: Morphology collapsed due to air-drying.

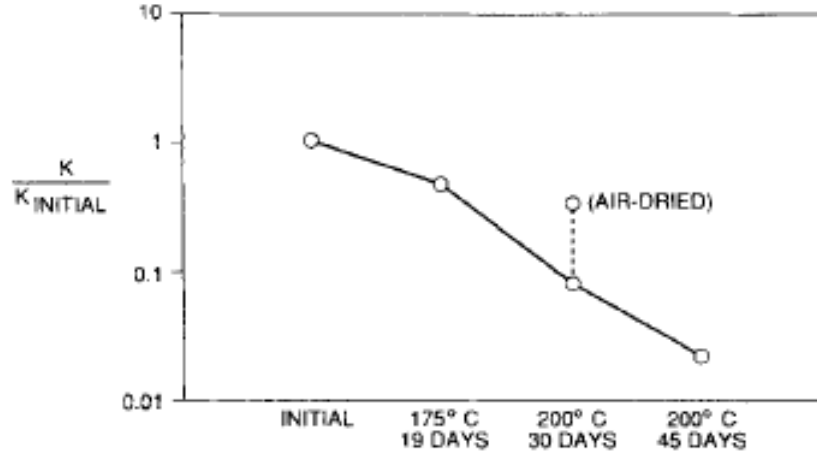


Figure 13: Normalized brine permeability vs. reaction progress. Note the effect of morphology collapse due to air-drying. Figure from [47].

decrease due to diagenetic clay minerals could prove to be a limiting factor on production.

## 4.2 CEC: effects of particle size and pH

The cation exchange capacity of a clay mineral is the product of the charge density and the available surface area. Although CEC is one of the parameters used to categorize clay minerals it can be highly dependent on particle dimensions and pH [51, 50, 3, 52, 25, 53]. The surface area can be subdivided into basal surface area and edge surface area. Referring to the kaolinite particle shown in figure 14, the basal surface area is the sum of the top and bottom surfaces of the crystal. The edge surface is the circumference of the particle multiplied by the thickness of the particle. Estimates of edge surface area are based on geometrical considerations and the aspect ratio of the clay particle, i.e. particle diameter to thickness. The dimensions of clay particles can be measured by transmission electron microscope (TEM) or scanning force microscopy (SFM).

In one study dimensions of fundamental particles of interstratified clays, illite, and smectites were recorded by a TEM shadowing technique [53]. Fundamental particles in this context means the thinnest particle unit possible for a mineral, a particle that can be achieved by complete dispersal in aqueous suspension. Drops of highly diluted suspension were placed on freshly cleaved mica, which provides an ultraflat surface. The mica was subsequently shadowed at an approximate angle of  $10^\circ$  by evaporated platinum and covered in a uniform coating of carbon. The resulting images are shown in figure 15. Thickness

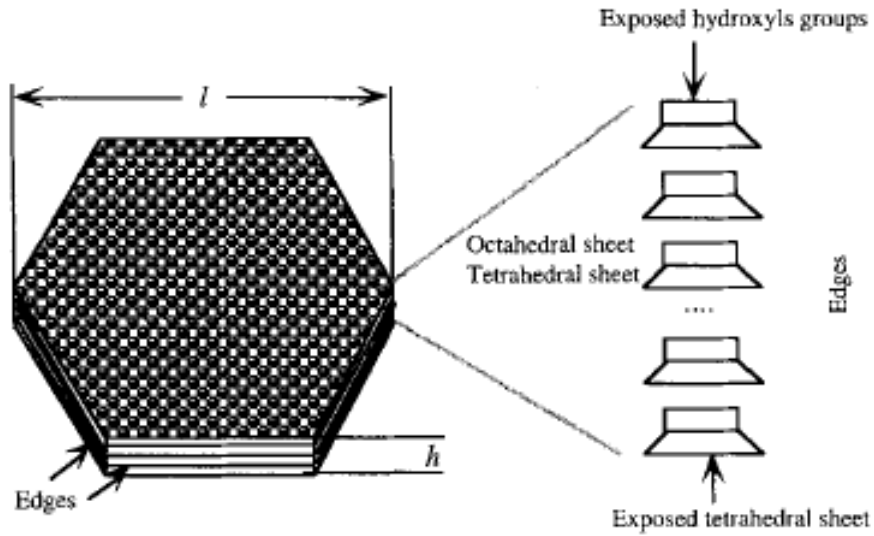


Figure 14: Simplified model of a kaolinite particle showing basal and edge surfaces. Thickness of the particle is denoted by  $h$ , diameter denoted by  $l$ . Figure from [50].

was determined from the images by applying equation (18).

$$T = (l * \tan\alpha) / m \quad (18)$$

Where

$T$  is the thickness of the fundamental particle

$l$  is the length of the shadow

$\alpha$  is the shadowing angle

$m$  is the magnification

Three-dimensional TEM analysis makes it possible to calculate basal surface area, edge surface area and total surface area of individual particles. Given a large enough sample size, the mean values can be used to calculate the surface area in  $\text{m}^2/\text{g}$  if the density of the mineral is known [53]. A correlation between total surface area and mean particle thickness is given in figure 16.

Edge and basal surface area can also be determined from SFM images. This method was used in a study which measured site densities of kaolinite from proton adsorption isotherms [51]. In this study kaolinite particle aggregates, as opposed to fundamental particles, were placed on freshly cleaved mica and allowed to air dry. The sample was then probed with conical silicon tips in order to generate SFM images for analysis. For their well crystallized kaolinite

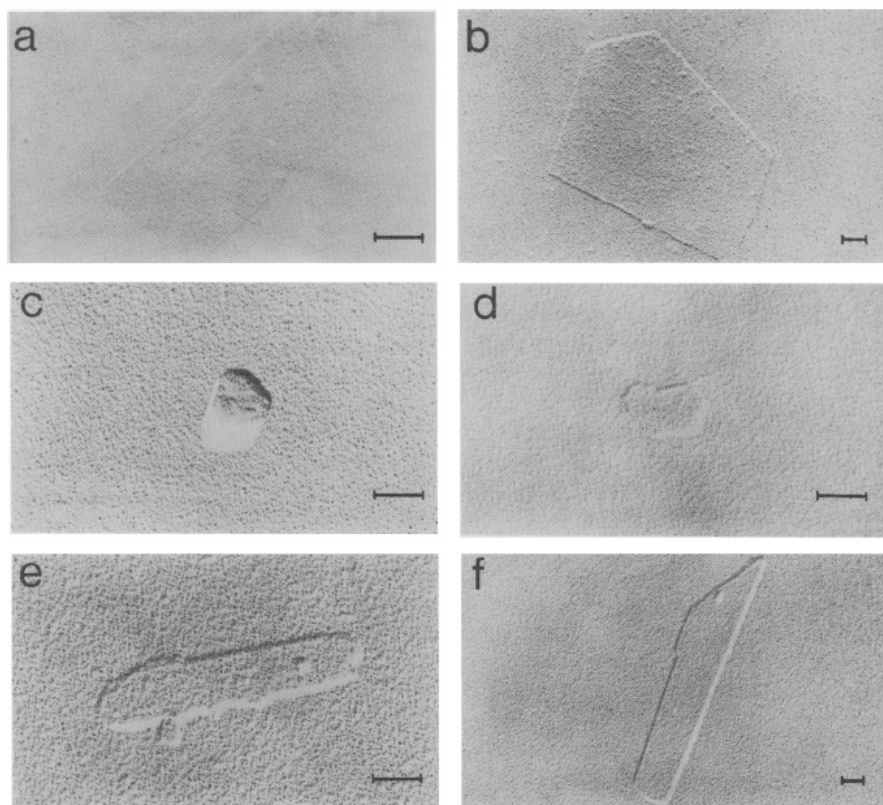


Figure 15: TEM images of platinum shadowed fundamental particles. A: Wyoming montmorillonite ; B: Na-rectorite, regularly interstratified paragonite-smectite. 50% paragonite layers; C: Interstratified kaolinite-smectite. 75% kaolinite layers; D: Synthetic mica-smectite. 70% mica layers; E: Interstratified illite-smectite. 80% illite layers; F: Illite. Scale bar is 0,1  $\mu m$  in all views. Figure from [53].

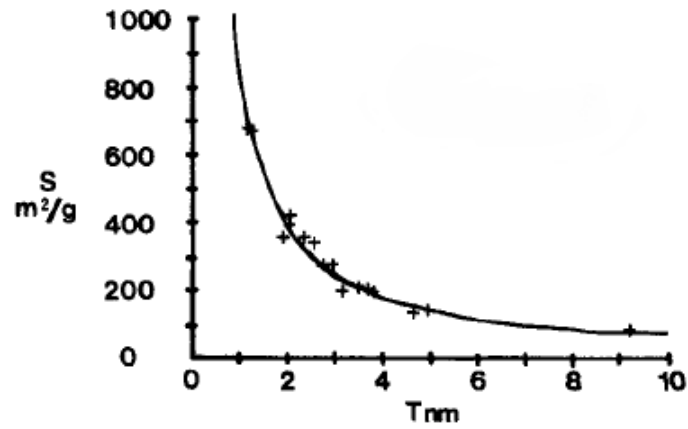


Figure 16: Total surface are vs. mean particle thickness. Curve corresponds to best fit:  $S = \frac{825}{T}$ . Figure modified from [53].

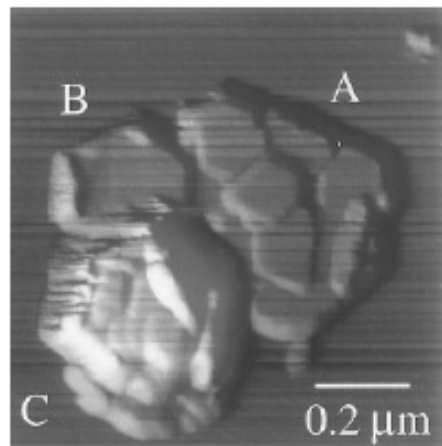


Figure 17: SFM image of kaolinite particles. The brightest area on particle c represents a height of 120 nm. Particle diameters are in the range of 50-600 nm. Figure from [51].

sample they found aspect ratios ranging from 2:1 to 10:1 and edge surface areas in the range of 10-50% of total surface area [51]. An SFM image of the kaolinite particles is shown in figure 17. Note that the basal surface is not flat, but have topographic variations due to overlying particles. This contributes to additional edge surface area of about 5% of total geometric surface area [51]. A titration against 0,1 M NaOH and 0,1 M HCl was carried out to determine surface charge on the clay at different pH and temperatures. Since lattice substitutions are minor and insignificant [51, 50] in kaolinite the authors assumed that all the surface charge should stem from silanol and aluminol sites on the edges and basal planes. As a result of the SFM image analysis, which found a higher edge surface area than was expected, the basal planes were not needed to account for the observed charge site densities [51]. The researchers suggest that the contribution of edge surface area is larger than previously thought. Similarly to the SFM study by Brady et al., kaolinite aspect ratios ranging from 2:1 to 10:1 were also found by another study [54]. It is hard to find a figure on montmorillonite aspect ratios, but SEM images from one study show particle diameters in excess of 500 nm. Using the common assumption that fully hydrated Na-montmorillonite is regarded as sheets of 1 nm, unit cell thickness [53, 54, 21] gives an estimate of 500:1. Using data from [53] I calculated the aspect ratio of the Wyoming montmorillonite. The required formula is given by equation (19):

$$AR = \frac{(L * W)^{\frac{1}{2}}}{T} \quad (19)$$

Where

$AR$  is the aspect ratio

$L$  is the length of the particle

$W$  is the width of the particle

$T$  is the thickness of the particle

Mean values of length, width, and thickness for the 34 samples plugged into the equation above yield an aspect ratio of 217:1.

A study of the hydrothermal growth habits of illitized smectite found that as the clay particles undergo “Ostwald ripening” their morphology changed from elongated, thin particles to hexagonal particles, growing at a constant aspect ratio of about 40:1 [56]. It was also observed that the frequency distributions of particle thickness became broader with increasing depth. The mean particle thickness increased from 5,9 nm for the 40 meter samples to 22,7 nm for the 290 meter sample [56]. A similar trend was observed for frequency distributions of equivalent diameter vs. depth, with broadening of the distribution and increase in mean value [56]. According to the theory of “Ostwald ripening” illite crystal growth rate is a function of supersaturation of illite in the pore solution. For a high porosity, fluid dominated medium, supersaturation of illite can be assumed nearly constant during ripening due to advective flux [56]. In essence this means

Clay mineral	Kaolinite	Chlorite	Illite	Montmorillonite
AR	2 : 1 – 10 : 1 [51, 54]	~ 20 : 1*	~ 50 : 1*	200 – 500 [53, 54, 51]
Surface area [m <sup>2</sup> /g]	10 – 150*	20*-140 [21]	50 – 400* [53]	100 – 800* [53]
Edge area [%]	20 – 30 [54, 51]	–	2 – 10 [53, 54]	≤ 1 [53, 54]
CEC [meq/100g]	1 – 15 [21, 50, 25, 55]	10 – 40 [21]	20 – 70* [48]	~ 100 [48, 25, 55]

Table 2: Characteristics of common clay minerals. References are listed in brackets below values. Star notation indicates that the value is wholly or partly based on personal correspondence with Paul H. Nadeau.

that growth rates do not decrease as particle dimensions increase, which may explain the skewness of the frequency distributions towards larger sizes with increasing illitization [56]. Equivalent diameter was calculated by equation (20).

$$D = 2\left(\frac{LW}{\pi}\right)^{\frac{1}{2}} \quad (20)$$

Where

$D$  is the equivalent diameter

$L$  is the length of the particle

$W$  is the width of the particle

Some important characteristics for common clay minerals have been compiled in table 2. Keep in mind that these values are estimates and that they can vary considerably depending on particle size, mineralogical purity, pH, and particle sizes. The CEC value of chlorite may need to be adjusted as the estimate of 40 meq/100 g seems slightly high and 20-30 meq/100 g may be more appropriate as an upper constraint.

It was mentioned in section 2.7.2 that the edge charges of of clay minerals are pH dependent due to reactions between silanol and aluminol groups on the edges, as well as exposed hydroxyl groups on the basal octahedral plane. It follows from equations (9) and (10) that under alkaline conditions these charges will be negative, adding to the permanent charge imposed by lattice substitutions. Going back to equation (8) it is evident that the negative edge charges will diminish, and positive charges will form, with decreasing pH as aluminol groups develop positive charges [25]. Since the total CEC of a clay mineral is dependent on the CEC contributions from both edges and basal surfaces it follows that CEC is a function of pH and ratio between total surface area to edge surface area. The ratio of total area to edge area is a function of the aspect ratio defined by equation (19). CEC for a given clay mineral should increase for increasing pH,

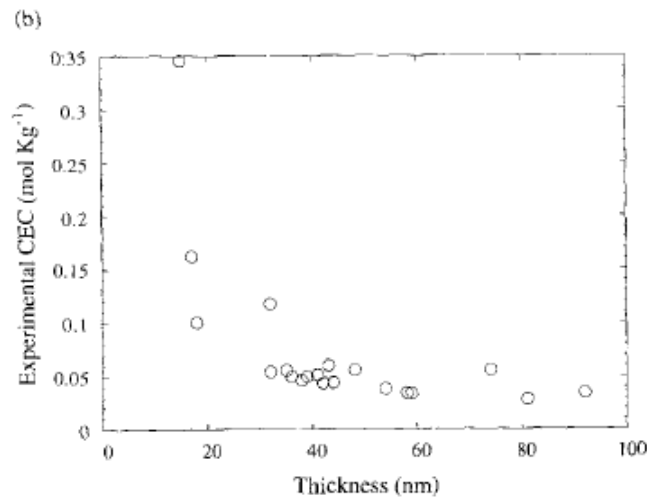
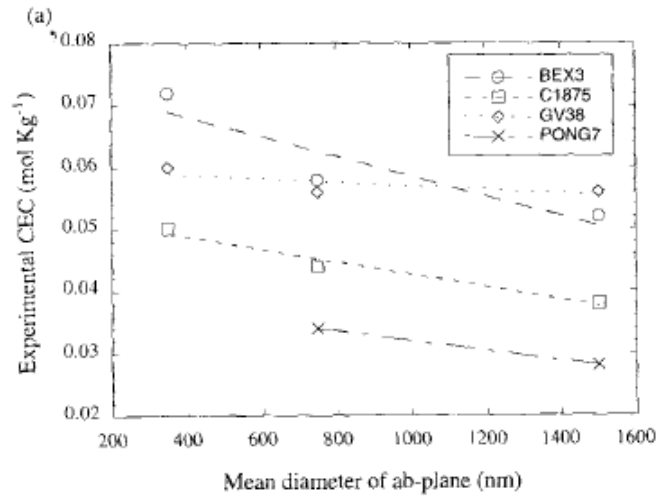


Figure 18: Variation in experimental CEC with respect to particle dimensions. A: CEC vs. mean plate diameter; B: CEC vs. particle thickness. Note that CEC is given in mol/kg. Figure from [50].



with clay minerals that have low aspect ratios being the most sensitive due to relatively higher edge surface area.

The relationship between particle size and CEC for kaolinite was described in a study that calculated theoretical CEC values and compared them to experimental measurements [50]. Figure 18 shows that the measured CEC for kaolinite increases with decreasing particle dimensions. Crystallinity was also discussed as a factor due to less crystalline kaolinite samples yielding a higher CEC. Poor crystallinity can be related to transport of the material and indicates a detrital origin [22]. However, the authors dismissed the crystallinity effect and attributed the deviation to the thinness of the poorly crystalline particles, again stating the effect of dimensions.

Regarding pH of sandstone reservoirs it is worth mentioning a correlation between  $\text{CO}_2$  and reservoir temperature proposed by Ehrenberg and Smith [57]. Identical linear correlations between temperature and the logarithm of the partial pressure of  $\text{CO}_2$  were found for the US Gulf Coast and the NSC. They suggested that the correlation was the result of inorganic chemical equilibria between feldspar, carbonate minerals, and clay. The correlation has the form of decreasing pH with higher temperature.

An often overlooked consequence of the pH dependent charges is that clay minerals also have anion exchange capacities, i.e. the ability to adsorb negatively charged ions. Like the CEC, this AEC is also a function of pH and edge area, with AEC increasing as pH decreases. It is an important property in soil science because it allows soil to adsorb anionic nutrient like  $\text{NO}_3^-$  and  $\text{PO}_4^{3-}$ . It might also play a part in adsorption/desorption of polar oil components for kaolinite and chlorite due to their relatively high edge surface area, and should be investigated further.

Temperature is another factor affecting the CEC of clay minerals. One study modelled kaolinite surface charge at different temperature and pH by combining potentiometric titration data, SFM-measured proportion of basal to edge area, and modelled surface charge density [51]. The resulting plot of surface charge versus pH and temperature is shown in figure 19. The researchers observed an increase in calculated site densities with increasing temperature, which may be due to production of additional surface area by dissolution of kaolinite [51]. Hydration and reactivity of cations such as  $\text{Ca}^{2+}$  and  $\text{Mg}^{2+}$  are also affected by temperature. By extension, the relative affinities for charge sites on the clay could be subject to deviations from the hierarchy that was established in section 2.7.2.

### 4.3 Initial wetting in sandstone reservoirs

In section 2.5 a brief review of oil components was given. During oil charge these polar components can adsorb onto the surface of the rock, changing its wetting state from strongly water wet to more intermediate wetting states [8, 7]. The stability of the water film that coats the rock surface is a complex relationship between a number of factors. Composition of the crude oil, composition of the brine and pH have been identified as factors that influence the stability of the

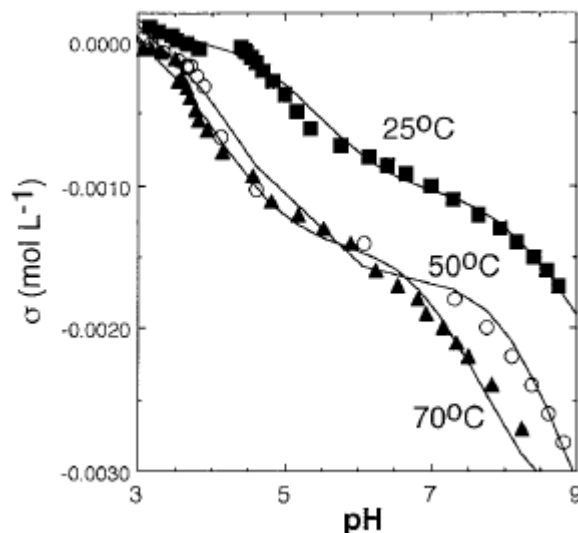


Figure 19: Modelled kaolinite surface charge vs. pH and temperature. Figure from [51].

film [7]. When it comes to film stability, temperature has an indirect effect as it has been observed that it influences the composition of crude oils. The acid number of oils has a negative relationship with temperature, probably due to decomposition of  $\text{-COOH}$  groups at high temperature [17].

At equal pH, increasing ionic strength (salinity) has been shown to generally decrease the adsorption of quinoline onto kaolinite, illite, and montmorillonite [3, 18, 17]. There was an exception for adsorption of quinoline onto montmorillonite at pH 9 in one of the cited studies which was explained by  $\text{Ca}^{2+}$  and  $\text{Mg}^{2+}$  acting as adsorption bridges between quinoline and the clay surface [17]. Increased adsorption with lower ionic strengths can easily be explained by the competition between cations and quinoline for the negative sites on the clay surface. Wettability experiments measuring contact angles have also shown increased oil wetness for lower ionic strengths, adding to the evidence that adsorption of polar components is higher for low ionic strength than it is for high ionic strengths at equal pH [7]. Figure 20 shows adsorption of quinoline onto illite in two brines of different salinity. Adsorption was found to be highest around the  $\text{pK}_a$  value of the base, which is about 4.9. The adsorption drops off with increasing alkalinity because of a decrease in the active, protonated form of the base. At  $\text{pH} < \text{pK}_a$  the adsorption falls due to increases competition from  $\text{H}^+$ . Increased recovery from wettability alteration is often observed in conjunction with increased pH, and pH has been shown to be the most important factor for adsorption of polar components onto clay in numerous experiments [17, 14, 3, 18].

It has been proposed that oil preferentially wets kaolinites in oil-saturated

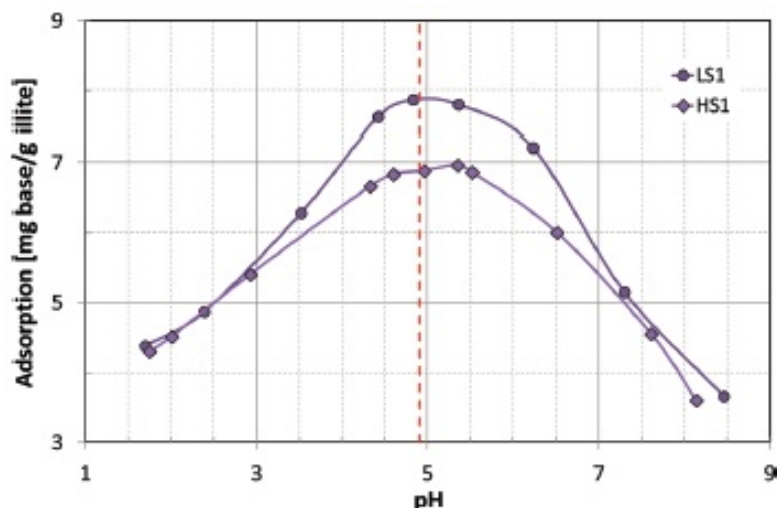


Figure 20: Adsorption of quinoline onto Illite in low saline (1000 ppm) and high saline (25000 ppm) brine. Dashed line indicates  $pK_a$  value of quinoline. Figure from [18].

sandstones while illites and other minerals are mainly wetted by water [58]. To test the validity of this claim an adsorption study was performed for asphaltenes onto three samples of kaolinite and three samples of illite, each with a specific genesis condition. Adsorption of water onto the clay samples was also measured in the same study. Results from the study showed that the hydrophilicity and adsorption differed significantly between the samples. While 28-38% of the illite surface area was found to be hydrophilic, only 25-28% of the kaolinite surface area exhibited hydrophilicity. Asphaltene adsorption ranged from 1,9-2,7  $\text{mg}/\text{m}^2$  for the kaolinite samples and from 0,3-1,7  $\text{mg}/\text{m}^2$  for the illites [58]. Most striking is the low asphaltene adsorption (0,3  $\text{mg}/\text{m}^2$ ) for the authigenic illite which was attributed to its high microporosity hindering access of the asphaltene to the surface. The authigenic illite also shows considerably less hydrophilicity than the two other illite samples. Cryo-SEM imaging (to prevent morphology collapse) of cores from the Brent formation, taken from depths of 3000-3600 m, have also shown interesting results with regards to clay minerals and wetting [59]. They found that not only the type and quantity, but also the morphology of the clay minerals in the core affected wetting distributions. Kaolinite showed higher affinity for oil than Illite did and in the core with the highest kaolinite content (7,8 wt%) the sample became oil-wet after ageing. Fibrous illite was shown to remain hydrophilic, showing no affinity for oil. Most interestingly, platy illite behaved more like kaolinite, becoming oil wet if the content was high enough [59]. This study suggests that morphology could play a part in initial wetting, with illite that has inherited a platy structure from the kaolinite it replaced yielding a more oil-wet state than fibrous illite.

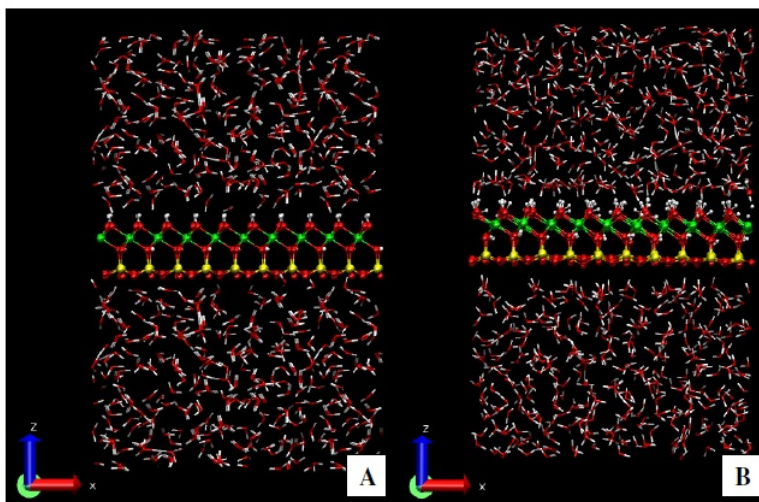


Figure 21: MDS of kaolinite basal planes. A: Initial condition; B: Equilibrium condition. Red: oxygen; Yellow: silicon; Green: aluminum; White: hydrogen. Figure from [55].

Regardless of the exciting implications, it should be noted that the sample sizes in these two studies are very small, and it would probably be unwise to attempt any generalization based on these results without further study of larger sample sizes.

It has also been suggested that the wettability of clay minerals is generally heterogenous and influenced by their crystal structure [55]. If lattice substitutions are minor or non-existent, the basal plane of the tetrahedral sheet will be electrically neutral and can be expected not to show much affinity for polar water molecules. The edges and octahedral planes however, have functional groups (OH, Si-OH, Al-OH, Mg-OH) which can undergo protonation and dissociation reactions, hence they are not electrically neutral. They can therefore be expected to have different wetting properties from the tetrahedral basal plane, something which was investigated in a recent PhD dissertation [55]. Results from the AFM study, conducted at pH 4, confirmed that the kaolinite silica face was moderately hydrophobic, with estimated advancing and receding contact angles of  $64^\circ$  and  $58^\circ$ , respectively. As expected the alumina face was found to be relatively hydrophilic. In addition to the AFM contact measurements, a molecular dynamics simulation (MDS) was carried out for a simulated kaolinite crystal placed in modelled water medium. A figure of the initial and equilibrium states are shown in figure 21. A significant difference between the two faces with regards to wetting is easily identified. Note the gap between the water phase and the tetrahedral face of the kaolinite. This gap is called the “exclusion zone” and is usually observed at hydrophobic surfaces. The difference in wetting characteristics can be explained by exposed hydroxyl groups which provide sites for

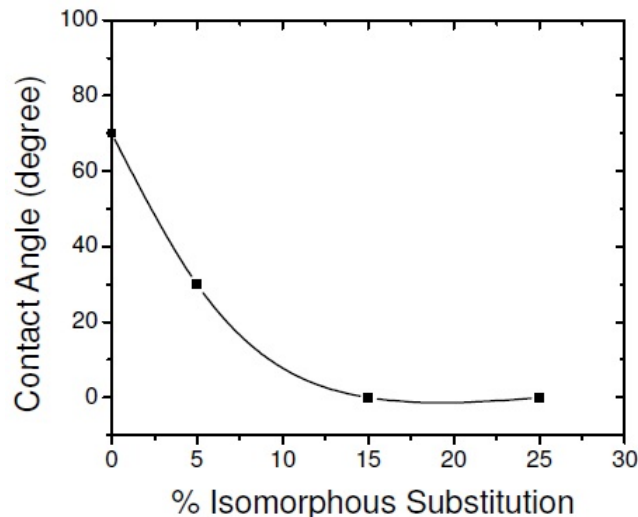


Figure 22: Water contact angle vs. degree of isomorphous substitution in silica tetrahedral for phyllosilicates. Figure from [55].

hydrogen bonding [55]. Yin also performed additional MDS simulations which studied contact angles as a function of isomorphous substitution in the tetrahedral sheets of phyllosilicates. The resulting plot is shown in figure 22. The data point at 15% substitution corresponds to the simulated Illite, it corroborates the belief that illite is naturally hydrophilic [55]. Clinocllore, a member of the chlorite family was also subjected to AFM study and determination of zeta potentials, charge densities, and surface potentials were carried out for three distinct surfaces. The surfaces in question were located on the tetrahedral silica sheet, the brucite-like sheet, and the edges, they were all measured pH values 5,6, 8 and 9. The tetrahedral face of the chlorite remained negatively charged for all values and exhibited little pH dependence. The brucite-like sheet retained its positive charge for all values but showed a stronger pH dependence. Edge surfaces had a positive charge of similar magnitude to the brucite-like sheet at pH 5,6 but show a strong pH dependence, reversing their charge between pH 8 and 9. At the end point of pH 9 it has a negative charge slightly less in magnitude than the tetrahedral sheet [55]. Yet again we find the explanation in the various protonation and deprotonation mentioned earlier.

#### 4.4 Conclusions: “Smart water” injection and pre-flood core studies

- Before smart water injections are carried out in a reservoir, appropriate screening criteria should be applied to ensure the viability of the injection fluid.

- When testing proceeds to core floods it is important that the conditions of the lab experiments are compatible with the actual reservoir state so that the benefits of the injections are neither overstated nor underestimated.
- If possible the cores should not be air-dried as this destroys the fibrous morphologies of illite and smectite, artificially increasing the permeability.
- During smart water injection simulations the crude oil and formation brine should be of the same or similar composition, and in the same state with respect to reservoir conditions (PPCO<sub>2</sub>, temperature, pH etc.) as in the subsurface.
- For reasons discussed in section 4.2, pH similarity is probably more important if the core has high amounts of kaolinite and chlorite than if the clay minerals are mainly illies or smectites.
- For adsorption/desorption studies where powdered clay samples are used it would be wise to consider the effect of particle size, especially for clay minerals with low aspect ratios.
- As discussed above that the degree of isomorphous substitution could be a factor in the initial wettability of the reservoir. If this is indeed the case, XRD analysis to determine the degree of substitution could be used to predictive tool.
- Because it could have implications for the potential of “smart water” injection, further experiments should be designed to investigate the possible links between crystal structure and wettability.
- Studies relating morphology and heritage to adsorption of polar component would also be interesting, as the data sets referred to in this thesis are lacking in size.
- Due to constraints on available literature and time this thesis has only briefly touched upon the subject of AEC, and it may warrant additional examination.

## References

- [1] *An industry for the future: Norway's petroleum activities*. Norwegian Ministry of Petroleum and Energy, 2011.
- [2] Y. Tormodsgard, ed., *Facts 2014 The Norwegian Petroleum Sector*. Norwegian Ministry of Petroleum and Energy and Norwegian Petroleum Directorate, 2014.
- [3] T. Austad, A. RezaeiDoust, and T. Puntervold, “Chemical mechanism of low salinity water flooding in sandstone reservoirs,” in *SPE Improved Oil Recovery Symposium, 24-28 April, Tulsa, Oklahoma, USA*, 2010.

- [4] K. Bjørlykke and P. Aagard, "Clay minerals in north sea sandstones," *SEPM Special Publication*, vol. 47, pp. 65–80, 1992.
- [5] D. W. Green and G. P. Willhite, *Enhanced Oil Recovery*. Society of Petroleum Engineers, 1998.
- [6] G. P. Willhite, *Waterflooding*, vol. 3. Society of Petroleum Engineers, 1986.
- [7] W. Abdallah, J. S. Buckley, A. Carnegie, B. Herold, J. Edwards, E. Fordham, A. Graue, T. Habashy, N. Seleznev, C. Signer, H. Hussain, B. Montaron, and M. Ziauddin, "Fundamentals of wettability," *Schlumberger Oilfield Review*, vol. 19, 2007.
- [8] W. G. Anderson, "Wettability literature survey- part 1: Rock/oil/brine interactions and the effects of core handling on wettability," *Journal of Petroleum Technology*, vol. 38, no. 10, pp. 1125–1144, 1986.
- [9] P. P. Jadhunandan and N. R. Morrow, "Effect of wettability on waterflood recovery for crude-oil/brine/rock systems," *SPE Reservoir Engineering*, vol. 10, pp. 40–46, 1995.
- [10] T. F. Moore and R. C. Slobod, "The effects of viscosity and capillarity on the displacement of oil by water," *Producers Monthly*, vol. 20, pp. 20–30, 1956.
- [11] A. Abrams, "The influence of fluid viscosity, interfacial tension, and flow velocity on residual oil saturation left by waterflood," *Society of Petroleum Engineers Journal*, vol. 15, pp. 437–447, 1975.
- [12] K. Kumar, E. Dao, and K. K. Mohanty, "Afm study of mineral wettability with reservoir oils," *Journal of Colloid and Interface Science*, vol. 289, pp. 206–217, 2005.
- [13] C. Pan, J. Feng, Y. Tian, L. Yu, X. Luo, G. Sheng, and J. Fu, "Interaction of oil components and clay minerals in reservoir sandstones," *Organic Geochemistry*, vol. 36, pp. 633–654, 2005.
- [14] A. RezaeiDoust, *Low Salinity Water Flooding in Sandstone Reservoirs: A Chemical Wettability Alteration Mechanism*. PhD thesis, University of Stavanger, 2011.
- [15] W. D. Burgos, N. Pisutpaisal, M. C. Mazzaresse, and J. Chorover, "Adsorption of quinoline to kaolinite and montmorillonite," *Environmental Engineering Science*, vol. 19, no. 2, pp. 59–68, 2002.
- [16] S. Strandal, J. Haavik, A. M. Blokhus, and A. Skauge, "Effect of polar organic components on wettability as studied by adsorption and contact angles," *Journal of Petroleum Science & Engineering*, vol. 24, pp. 131–144, 1999.

- [17] A. RezaeiDoust, P. T., and T. Austad, “Chemical verification of the eor mechanism by using low saline/smart water in sandstone,” *Energy & Fuels*, vol. 25, pp. 2151–2162, 2011.
- [18] H. Aksulu, D. Håmsø, S. Strand, T. Puntervold, and T. Austad, “Evaluation of low-salinity enhanced oil recovery effects in sandstone: Effects of the temperature and ph gradient,” *Energy & Fuels*, vol. 26, pp. 3497–3503, 2012.
- [19] S. Guggenheim and R. T. Martin, “Definition of clay and clay mineral: Joint report of the aipea nomenclature and cms nomenclature committees,” *Clay and Clay Minerals*, vol. 43, no. 2, pp. 255–256, 1995.
- [20] P. H. Nadeau and H. A., “Clay microporosity in reservoir sandstones: An application of quantitative electron microscopy in petrophysical evaluation,” *AAPG Bulletin*, vol. 79, no. 4, pp. 563–573, 1995.
- [21] International Drilling Fluids Limited, *Clay Chemistry, Technical Manual for Drilling, Completion and Workover Fluids*, 1982.
- [22] M. D. Wilson and E. D. Pittman, “Authigenic clays in sandstones: Recognition and influence on reservoir properties and paleoenvironmental analysis,” *Journal of Sedimentary Petrology*, vol. 47, no. 1, pp. 3–31, 1977.
- [23] R. Worden and S. Moras, eds., *Clay Mineral Cements in Sandstones: (Special Publication 34 of the IAS)*. 2002.
- [24] S. N. Ehrenberg, “Relationship between diagenesis and reservoir quality in sandstones of the garn formation, haltenbanken, mid-norwegian continental shelf,” *AAPG Bulletin*, vol. 74, no. 10, pp. 1538–1558, 1990.
- [25] E. Tombácz and M. Szekeres, “Surface charge heterogeneity of kaolinite in aqueous suspension in comparison with montmorillonite,” *Applied Clay Science*, vol. 34, pp. 105–124, 2006.
- [26] P. H. Nadeau and R. C. J. Reynolds, “Burial and contact metamorphism in the mancos shale,” *Clay and Clay Minerals*, vol. 29, no. 4, pp. 249–259, 1981.
- [27] K. Bjørlykke, A. P., H. Dypvik, D. S. Hastings, and A. S. Harper, “Diagenesis and reservoir properties of jurassic sandstones from the haltenbanken area, offshore mid-norway,” in *Habitat of Hydrocarbons on the Norwegian Continental Shelf: Proceedings of an International Conference (Habitat of Hydrocarbons, Norwegian Oil and Gas Finds)*, 1986.
- [28] S. N. Ehrenberg and P. H. Nadeau, “Formation of diagenetic illite in sandstones of the garn formation, haltenbanken area, mid-norwegian continental shelf,” *Clay Minerals*, vol. 24, no. 2, pp. 233–253, 1989.



- [29] K. Bjørlykke, T. Nedkvitne, M. Ramm, and G. C. Saigal, “Diagenetic processes in the brent group (middle jurassic) reservoirs of the north sea: an overview,” *Geological Society Special Publications*, vol. 61, pp. 263–287, 1992.
- [30] “petrowiki.org/waterflooding.” Accessed 07.06.2014.
- [31] J. C. Martin, “The effects of clay on the displacement of heavy oil by water,” in *Venezuelan Annual Meeting, 14-16 October, Caracas, Venezuela*, 1959.
- [32] G. G. Bernard, “Effect of floodwater salinity on recovery of oil from cores containing clays,” in *SPE California Regional Meeting, 26-27 October, Los Angeles, California*, 1967.
- [33] A. Lager, K. J. Webb, C. J. J. Black, M. Singleton, and K. S. Sorbie, “Low salinity oil recovery - an experimental investigation,” *Petrophysics*, vol. 49, pp. 28–35, 2008.
- [34] A. Lager, K. J. Webb, I. R. Collins, and D. M. Richmond, “Local enhanced oil recovery: Evidence of enhanced oil recovery at the reservoir scale,” in *SPE Symposium on Improved Oil Recovery, 20-23 April, Tulsa, Oklahoma, USA*, 2008.
- [35] D. J. Ligthelm, J. Gronsveld, J. P. Hofman, N. J. Brussee, F. Marcelis, and H. A. van der Linde, “Novel waterflood strategy by manipulation of injection brine composition,” in *EUROPEC/EAGE Conference and Exhibition, 8-11 June, Amsterdam, The Netherlands*, 2009.
- [36] G.-Q. Tang and N. R. Morrow, “Oil recovery by waterflooding and imbibition - invading brine cation valency and salinity,” in *Proceedings of the International Symposium of the Society of Core Analysts, Golden, CO*, 1999.
- [37] G.-Q. Tang and N. R. Morrow, “Influence of brine composition and fines migration on crude oil/brine/rock interactions and oil recovery,” *Journal of Petroleum Science & Engineering*, vol. 24, pp. 99–111, 1999.
- [38] A. Lager, K. J. Webb, and C. J. J. Black, “Impact of brine chemistry on oil recovery,” in *14th European Symposium on Improved Oil Recovery, Cairo, Egypt, 2006.*, 2006.
- [39] Y. Zhang, X. Xie, and N. R. Morrow, “Waterflood performance by injection of brine with different salinity for reservoir cores,” in *SPE Annual Technical Conference and Exhibition, Anaheim, CA, USA.*, 2007.
- [40] P. I. McGuire, J. R. Chatham, F. K. Paskvan, D. M. Sommer, and F. H. Carini, “Low salinity oil recovery: An exciting new opportunity for alaska’s north slope,” in *SPE Western Regional Meeting, 30 March-1 April, Irvine, California*, 2005.

- [41] P. A. Bjørkum and P. H. Nadeau, "Temperature controlled porosity/permeability reduction, fluid migration, and petroleum exploration in sedimentary basins," *APPEA Journal*, vol. 38, pp. 453–464, 1998.
- [42] P. H. Nadeau and A. Hurst, "Application of back-scattered electron microscopy to the quantification of clay mineral microporosity in sandstones," *Journal of Sedimentary Petrology*, vol. 61, no. 6, pp. 921–925, 1991.
- [43] P. H. Nadeau, "Earth's energy "golden zone": a synthesis from mineralogical research," *Clay Minerals*, vol. 46, pp. 1–24, 2011.
- [44] E. H. Oelkers, P. A. Bjørkum, and W. M. Murphy, "A petrographic and computational investigation of quartz cementation and porosity reduction in north sea sandstones," *American Journal of Science*, vol. 296, no. 4, pp. 420–452, 1996.
- [45] S. N. Ehrenberg, "Preservation of anomalously high porosity in deeply buried sandstones by grain-coating chlorite: Examples from the norwegian continental shelf," *AAPG Bulletin*, vol. 77, no. 7, pp. 1260–1286, 1993.
- [46] P. H. Nadeau and S. Hillier, "A geological model for diagenetic chlorite coated sandstone reservoirs, permeability, water saturation, porosity preservation, and field development strategies.," in *Frontiers in Diagenesis: Clay and carbonate facies and their diagenetic pathways in reservoir rocks*, 2011.
- [47] P. H. Nadeau, "An experimental study of the effects of diagenetic clay minerals on reservoir sands," *Clays and Clay Minerals*, vol. 46, no. 1, pp. 18–26, 1998.
- [48] P. H. Nadeau and D. C. Bain, "Composition of some smectites and diagenetic illitic clays and implications for their origin," *Clays and Clay Minerals*, vol. 34, no. 4, pp. 455–464, 1986.
- [49] J. Alvarez and S. Han, "Current overview of cyclic steam injection process.," *Journal of Petroleum Science Research*, vol. 2, no. 3, pp. 116–127, 2013.
- [50] C. Ma and R. A. Eggleton, "Cation exchange capacity of kaolinite," *Clays and Clay Minerals*, vol. 47, no. 2, pp. 174–180, 1999.
- [51] P. V. Brady, R. T. Cygan, and K. L. Nagy, "Molecular controls on kaolinite surface charge," *Journal of Colloid and Interface Science*, vol. 183, pp. 356–364, 1996.
- [52] P. H. Nadeau, "Relationships between the mean area, volume and thickness for dispersed particles of kaolinites and micaceous clays and their application to surface area and ion exchange properties," *Clay Minerals*, vol. 22, pp. 351–356, 1987.

- [53] P. H. Nadeau, "The physical dimensions of fundamental clay particles," *Clay Minerals*, vol. 20, pp. 499–514, 1985.
- [54] J. Wan and T. K. Tokunaga, "Partitioning of clay colloids at air-water interfaces," *Journal of Colloid and Interface Science*, vol. 247, pp. 54–61, 2002.
- [55] X. Yin, *ANISOTROPIC SURFACE FEATURES OF SELECTED PHYLLOSILICATES*. PhD thesis, University of Utah, 2012.
- [56] A. Inoue and R. Kitagawa, "Morphological characteristics of illitic clay minerals from a hydrothermal system," *American Mineralogist*, vol. 79, pp. 700–711, 1994.
- [57] S. N. Ehrenberg and J. T. Smith, "Correlation of carbon dioxide abundance with temperature in clastic hydrocarbon reservoirs: relationship to inorganic chemical equilibrium," *Marine and Petroleum Geology*, vol. 6, pp. 129–135, 1989.
- [58] A. Saada, B. Siffert, and E. Papier, "Comparison of the hydrophilicity/hydrophobicity of illites and kaolinites," *Journal of Colloid and Interface Science*, vol. 174, no. 1, pp. 185–190, 1995.
- [59] C. Durand and E. Rosenberg, "Fluid distribution in kaolinite- or illite-bearing cores. cryo-sem observations versus bulk measurements.," *Journal of Petroleum Science & Engineering*, vol. 19, pp. 65–72, 1998.